Neutrophil Extracellular Traps Drive Inflammation in Local Skin and Distant Kidneys in UVB-Irradiated Lupus-Prone Mice

Xing Lyu[1,2,4], Minghui Yi[1,2,], Minghui Li[1,2,4], Ping L. Zhang[3], Wei Wei[,4], Victoria P. Werth[1,2*], Ming-Lin Liu[1,2*]

[1] Corporal Michael J. Crescenz VAMC, Philadelphia, PA, USA
[2] Department of Dermatology, Perelman School of Medicine, University of Pennsylvania, Philadelphia, PA, USA
[3] Division of Anatomic Pathology, Beaumont Laboratories, Beaumont Health, Royal Oak, Michigan 48073, USA
[4] Department of Rheumatology and Immunology, Tianjin Medical University General Hospital, Tianjin, China

Short title: NETosis drives UVB-induced lupus skin and kidney inflammation

Correspondence to: Ming-Lin Liu, MBBS, PhD, and Victoria P. Werth, MD, Department of Dermatology, Perelman School of Medicine, University of Pennsylvania, and Philadelphia Veterans Administration Medical center. Room B414, 3900 Woodland Avenue, Philadelphia, PA 19104, eMAIL: lium1@pennmedicine.upenn.edu; werth@pennmedicine.upenn.edu

Key words: SLE, NETosis, PKCα, CXCR4, Skin-kidney communication,

Word count
Main text: 6423
Abstract: 255
Significance: 117
Figures: 7
Suppl Figures: 3
References: 66

ABSTRACT

Sunlight is a primary environmental trigger for systemic lupus erythematosus (SLE). However, the mechanisms linking cutaneous inflammation to internal organ damage remain poorly defined. Here, we identify a critical role for neutrophil extracellular trap (NET) formation in a pathogenic skin-kidney axis that drives UVB-induced lupus skin and kidney inflammation. In asymptomatic lupus-prone mice, UVB irradiation elicited concurrent skin and kidney inflammation, characterized by neutrophil infiltration, NET formation, release of NET-associated cytokines and complement C3, and proteinuria. Importantly, targeting nuclear envelope rupture—a critical structural step enabling nuclear chromatin release during NETosis—through Pkcα genetic deletion significantly attenuated NET formation, skin and kidney inflammation, and proteinuria in UVB-irradiated MRL/*lpr;Pkcα*$^{-/-}$ mice. Beyond local NETosis, UVB primed skin-infiltrating neutrophils to express the migration receptor CXCR4 alongside proinflammatory cytokines and C3. Using spatiotemporal tracking via photoconversion, we revealed that non-NETting, CXCR4-expressing neutrophils migrated from the skin to the kidneys, where they subsequently underwent NETosis to release their pre-expressed cytokines and C3, thereby driving renal inflammation and injury. Genetic Cxcr4 deficiency impaired this inter-organ trafficking, attenuating renal neutrophil infiltration and proteinuria in UVB-irradiated *kikGR;Cxcr4*$^{+/-}$ mice. Pharmacological CXCR4 inhibition further validated the therapeutic potential of blocking this migratory axis, attenuating lupus skin and kidney inflammation in UVB-irradiated lupus-prone mice. By linking environmental UVB exposure to systemic lupus outcomes through PKCα-driven nuclear envelope rupture for proinflammatory NET release and CXCR4-mediated neutrophil trafficking for systemic dissemination, this work provides strong mechanistic evidence for a skin-kidney axis in SLE. These findings identify nuclear envelope regulation and neutrophil trafficking as previously underexplored therapeutic targets for photosensitive SLE.

SIGNIFICANCE

This study explores a mechanistic skin-kidney axis in SLE, revealing a causal link between UVB-induced cutaneous inflammation and systemic disease exacerbations. We demonstrate that PKCα-driven nuclear envelope rupture is critical for the release of proinflammatory NETs, while CXCR4-mediated trafficking of non-NETting neutrophils represents a pivotal route for systemic dissemination. These findings delineate how neutrophils transition from local initiators of skin inflammation to systemic effectors of renal injury by propagating NET-driven inflammatory cascades. This work suggests a shift in the therapeutic paradigm toward precise regulation of neutrophil migration and NETosis kinetics. By uncovering these underexplored pathways, the study provides a molecular framework for intercepting UVB-induced systemic exacerbation in photosensitive SLE, with the potential to mitigate irreversible end-organ damage.

INTRODUCTION

Systemic lupus erythematosus (SLE) is a systemic autoimmune disease characterized by inflammatory damage to multiple organs, such as the skin and kidneys. The pathogenesis of SLE involves the accumulation of immune cells, cytokines, immune complexes (ICs), and complement, which drives inflammatory responses and irreversible tissue damage (1). While the etiology remains a complex interplay of genetic, epigenetic, and environmental factors (1, 2), the discordance of SLE in monozygotic twins, who share nearly identical DNA, highlights the crucial role of environmental triggers (1).

Since the 1960s, sunlight has been recognized as a primary environmental trigger for lupus flares (3). Over 70% of patients with cutaneous lupus erythematosus (CLE) are photosensitive (4), where ultraviolet B (UVB) overexposure exacerbates both local skin inflammation and systemic symptoms, such as lupus nephritis, in SLE patients and autoimmune mice (5-8). Epidemiological studies from regions with high sun exposure further confirm a seasonal pattern for severe manifestations like lupus nephritis (9,10). Despite this clear clinical link, the precise mechanisms by which cutaneous UVB exposure leads to systemic inflammation and distant internal organ injury remain a critical knowledge gap in SLE pathogenesis.

Neutrophils are the first circulating leukocytes to infiltrate the skin following UVB overexposure (11) and act as the primary initiator immune cells in the pre-lesional skin, driving the development of early spontaneous CLE lesions in a new lupus mouse model (12). We previously demonstrated that UVB irradiation triggers skin inflammation and neutrophil infiltration, with a fraction of these cells undergoing NETosis—the release of neutrophil extracellular traps (NETs) (13,14). Notably, NETosis plays an important role in the pathogenesis of skin lupus (15,16) and lupus nephritis (17, 18). NETs are potent inducers of type I interferon (IFN-I) (14,19), a primary driver of lupus pathogenesis (20). Furthermore,

both NETs and IFN-I can induce B cell activation and proliferation (21,22), leading to autoantibody production and IC formation (23). NETs also serve as critical scaffolds for complement activation, amplifying tissue damage and driving lupus inflammation (24,25). Thus, the deposition of ICs and C3 in the skin (26) or kidneys (27) contributes to inflammatory responses and tissue damage in these organs. Importantly, accumulating evidence indicates that histones can directly induce NETosis (28), and that NET-releasing neutrophils can induce secondary NETosis in nearby naive neutrophils, thereby amplifying inflammatory signaling (29). Consistent with this, recent *in vivo* work demonstrated a delayed second wave of NET formation in the liver, driven by residual NET components from the first wave several days after LPS injection (30). Thus, neutrophil NETs function not only as effectors but also as self-propagating mediators of inflammation. This self-sustaining nature underscores the central role of NETosis in the systemic autoimmune cascades characteristic of SLE.

Building on our established model of UVB-induced skin inflammation with NET formation (13,14), we investigated NETosis in systemic lupus inflammation using asymptomatic, young female lupus-prone mice. UVB triggered concurrent skin and kidney inflammation, characterized by NET formation, release of NET-associated cytokines and complement, and proteinuria. This model mimics sunlight-triggered lupus flares in patients (6). Notably, UVB induces skin production of platelet-activating factor (PAF) (31), which triggers PKCα activation in neutrophils (32). Based on our discovery that PKCα drives nuclear envelope rupture—a critical structural step required for NET release via nuclear lamina phosphorylation and disassembly (13)—we investigated whether targeting nuclear envelope rupture through Pkcα deletion could attenuate UVB-induced skin and kidney inflammation in lupus-prone mice. Moreover, UVB primed skin-infiltrating neutrophils to express CXCR4, enabling the transmigration of non-NETting neutrophils from skin to kidneys. Using *in vivo* spatiotemporal photoconversion tracking, we showed that genetic Cxcr4 deletion blocked

neutrophil transmigration from inflamed skin to the kidneys, reducing renal inflammation in a non-lupus strain. Pharmacological CXCR4 inhibition confirmed these findings in UVB-irradiated lupus-prone mice.

By elucidating mechanistic evidence for a skin-kidney axis driven by PKCα-mediated NETosis and CXCR4-guided neutrophil transmigration, this study links environmental triggers to systemic lupus pathogenesis. These findings identify nuclear envelope modulation and neutrophil trafficking as therapeutic targets for preventing sunlight-triggered systemic lupus exacerbation, shedding light on previously underexplored mechanisms and offering new therapeutic strategies for photosensitive SLE.

RESULTS

UVB exposure triggered concurrent skin and kidney inflammation with neutrophil infiltration and NET release in asymptomatic young female lupus-prone mice. Exposure of asymptomatic, young female lupus-prone mice to UVB (Fig 1A) elicited skin inflammation, characterized by increased epidermal and dermal thickness and substantial inflammatory cell infiltration (quantified as nucleated cell count) (Fig 1B-E) compared to non-irradiated sham controls. Remarkably, this local skin UVB irradiation also triggered a systemic response, manifesting as acute renal injury with significant proteinuria and glomerular hypercellularity (Fig 1F-H) compared to sham controls. Further analyses demonstrated that UVB-induced skin inflammation was characterized by robust neutrophil infiltration (Fig 1I) and NET formation (Fig 1J,K) in MRL/*lpr* mice compared to sham controls. Notably, these skin-infiltrating neutrophils and their released NETs were highly enriched with proinflammatory cytokines, including IFNα, IFNγ, IL-17A, and C3 (Fig 1L-O), thereby establishing NETs as critical reservoirs of pro-inflammatory mediators in UVB-challenged skin of lupus-prone mice.

Crucially, we observed a potent correlation between the magnitude of skin inflammation and the severity of systemic disease. Specifically, the severity of cutaneous inflammatory cell infiltration (nucleated cell count) correlated significantly with systemic renal disease (proteinuria severity, Fig 1P). This systemic impact is further highlighted by the correlation between skin neutrophil infiltration and proteinuria (Fig 1Q). Collectively, these findings suggest that skin-infiltrating immune cells, particularly neutrophils, are not merely local responders but critical pathogenic drivers of systemic disease progression, potentially mediating an inflammatory cascade from the skin to the kidneys.

Although previous studies have implicated neutrophils in systemic injury following skin thermal burns (33,34) or UVB exposure (35), the molecular mechanisms linking cutaneous UVB damage to distant organ damage remain unclear. Since neutrophil NETosis has been shown to contribute to both UVB-induced skin inflammation (13,14) and lupus-associated nephritis (17,18) through the presentation of proinflammatory mediators, our findings suggest that UVB-triggered neutrophil infiltration and NETosis play a critical role in bridging local cutaneous injury and distant renal inflammation in lupus-prone mice. We therefore investigated the specific role of neutrophil NETosis in mediating inflammation in the skin and kidney.

Neutrophil NETosis drives acute kidney inflammation in lupus-prone mice following UVB irradiation. Beyond the cutaneous response (Fig 1I-O), we found that glomerular neutrophil infiltration correlated with glomerular hypercellularity in the combined groups of MRL/lpr mice without or with UVB irradiation (Suppl Fig 1A). This suggests a contribution of glomerular neutrophil infiltration to glomerular hypercellularity and renal inflammation. In addition, UVB-irradiated MRL/*lpr* mice exhibited significant glomerular neutrophil infiltration and a robust accumulation of neutrophil NETs—marked by citrullinated H3 (citH3)—compared to sham controls (Fig 2A-C). Crucially, these glomerular NETs acted as

potent drivers of acute renal injury, co-localizing with elevated glomerular levels of NET-associated proinflammatory cytokines (IFNα, IFNγ, IL-17A), and C3 (Fig 2D-H). The pathological relevance of this accumulation was underscored by potent positive correlations between the levels of glomerular neutrophils, NETs, IFNα, IFNγ, IL-17A, and C3 and the severity of proteinuria in the combined group of MRL/*lpr* mice (Fig 2I-K, Suppl Fig 1B-D). These results directly link these neutrophil NETs, their associated cytokines, and C3 to acute renal inflammation and injury following UVB exposure.

Thus, our findings highlight a key role for infiltrating neutrophils and their released NETs in driving multi-organ inflammation in the skin and kidneys following localized UVB irradiation. Notably, through the release of NETs and associated inflammatory mediators, neutrophils act as critical drivers of coordinated inflammatory responses in both the skin and kidneys of asymptomatic lupus-prone mice. Taken together, the coordinated responses of neutrophil activation and NET formation observed in both organs (Figs 1-2, Suppl Fig 1) suggests a direct mechanistic link between cutaneous and kidney inflammation.

Targeting nuclear envelope rupture via PKCα genetic deletion attenuated NETosis and UVB-induced lupus skin inflammation in MRL/*lpr* mice with Pkcα deficiency. NETosis is an established driver of lupus pathogenesis (15,36,37)—including in UVB-triggered skin and kidney inflammation (Figs 1-2)—yet the upstream mechanism controlling NET release *in vivo* remains elusive. While peptidyl arginine deiminase 4 (PAD4) has been considered a key therapeutic target for NETosis-related diseases, studies in lupus models challenge its necessity. In MRL/*lpr* mice, genetic Pad4 deletion failed to mitigate systemic disease, nephritis, or skin inflammation (38), indicating PAD4-independent mechanisms. Our recent study identifies that PKCα-mediated nuclear lamin B phosphorylation and disassembly drive nuclear envelope rupture, nuclear chromatin release, and subsequent NET formation (13,37). Thus, the PKCα-

Lamin B axis represents a fundamental mechanical requirement for nuclear chromatin release during NETosis. Based on this mechanism (13), we generated lupus-prone mice with a genetic deletion of Pkcα to investigate the effects of controlling NETosis on UVB-induced lupus skin and kidney inflammation.

Following UVB irradiation, MRL/*lpr;Pkcα*$^{-/-}$ mice (Fig 3A) exhibited a marked reduction in lupus skin inflammation compared to MRL/lpr mice, as demonstrated by significantly reduced epidermal and dermal skin thickness, lower nucleated cell counts, and diminished neutrophil infiltration (Fig 3B-D). Notably, UVB irradiation triggered significantly less neutrophil NETosis (Fig 3E) in Pkcα-deficient lupus-prone mice, which corresponded with a significant reduction in the accumulation of NET-associated proinflammatory factors, including IFNα, IFNγ, IL-17A, and C3, in the skin (Fig 3F-K). This model provides the first *in vivo* evidence that regulating nuclear envelope integrity by abolishing PKCα effectively suppresses NETosis and mitigates lupus-related tissue damage. These findings also confirm the critical role of neutrophil NETs and their associated proinflammatory mediators in driving lupus cutaneous pathology, highlighting nuclear envelope regulation as a novel and potent therapeutic strategy for NETosis-driven lupus skin inflammation.

Targeting PKCα-nuclear envelope pathway suppressed NETosis and ameliorated UVB-induced acute kidney inflammation in MRL/*lpr* mice. Beyond its cutaneous effects, our findings demonstrate the profound systemic therapeutic potential of modulating nuclear envelope integrity. Genetically deleting PKCα to stabilize nuclear envelope integrity and inhibit NETosis significantly decreased UVB-induced acute kidney inflammation and proteinuria (Fig 4A-D) in lupus-prone mice. This novel intervention led to marked histological improvements, including reduced glomerular hypercellularity (Fig 4B-C) and attenuated neutrophil infiltration in their kidneys (Fig 4D). Critically, we observed a profound reduction

in glomerular deposition of neutrophil NETs and their associated pathogenic cargo—including IFNα, IFNγ, IL-17A, and C3—in the kidneys of UVB-irradiated MRL/*lpr;Pkcα*$^{-/-}$ mice compared to MRL/*lpr* mice (Fig 4E-I). These findings provide definitive genetic evidence that the glomerular deposition of NETs and their associated pathogenic cargo are primary drivers of kidney injury and proteinuria (Fig 2I-K), establishing targeted regulation of NETosis as a promising therapeutic avenue for photosensitive lupus. Our study demonstrates a novel mechanistic paradigm by positioning nuclear envelope integrity as a promising therapeutic target for NETosis and NET-related pathologies, including lupus.

While our data confirm that NETotic neutrophils are essential end-effectors of kidney injury, prior studies demonstrate that only a portion of neutrophils undergo NETosis *in vitro* (39,40) and in the skin of UVB-irradiated mice *in vivo* (14). This raises the possibility that surviving, non-NETting neutrophils may serve as a migratory cellular bridge, facilitating systemic communication between the inflamed skin and distant kidneys following UVB irradiation (35). We therefore sought to delineate the mechanistic basis of this neutrophil-mediated cutaneous-renal interaction, exploring how these cells orchestrate NET release with pro-inflammatory cytokines/complement, and systemic inflammation following UVB irradiation.

UVB irradiation induced a migratory and pro-inflammatory neutrophil phenotype in lupus-prone mice. To address how local skin inflammation triggers distant organ injury, our findings identify CXCR4-expressing neutrophils as a critical cellular bridge to facilitate inter-organ communication during this systemic exacerbation. As a chemokine receptor, CXCR4 is known to facilitate communication between different organs by mediating the reverse transmigration (RTM) of immune cells, including neutrophils (41,42). Moreover, increased

CXCR4 expression on immune cells in SLE patients and lupus-prone mouse models supports its role in lupus development (43-48).

Strikingly, we observed a systemic elevation of CXCR4 expressing neutrophils following UVB irradiation in infiltrated skin and kidney neutrophils (regardless of NETotic states) and within their released NETs in MRL/*lpr* mice, compared to sham controls (Fig 5A-D). Importantly, the number of CXCR4-expressing neutrophils in the peripheral blood of UVB-irradiated mice was also significantly elevated (Fig 5E,F). Therefore, these systemic elevations of CXCR4-expressing neutrophils following UVB irradiation suggest the critical role of CXCR4 in facilitating communication between the inflamed skin and the kidneys.

To better understand this process, we exposed isolated neutrophils from these MRL/*lpr* mice directly to UVB or stimulated them with PAF, a lipid mediator released from keratinocytes after UVB irradiation (31). We observed that both UVB and PAF upregulated CXCR4 expression in mouse neutrophils in a dose-dependent manner (Fig 5G). This upregulation was accompanied by elevated expression of key inflammatory mediators, including IFNγ, IL-17A, and C3, as well as IFNα (in the presence of DNA-NETs, as previously characterized (13, 14)) (Suppl Fig 2A-D). Crucially, a subset of these primed neutrophils co-expressed CXCR4 alongside proinflammatory mediators (Fig 5H-O). These data demonstrate that UVB exposure—acting both directly and indirectly via PAF—reprograms skin-infiltrating neutrophils, empowering them with a dual migratory-inflammatory capability.

Therefore, the co-expression of CXCR4 and cytokines/C3 enables specific neutrophil subsets to mediate systemic migration from inflamed skin to the kidneys. Recognizing that only a fraction of neutrophils undergoes NETosis—both *in vitro* (39,40) and *in vivo* in the skin of UVB-irradiated mice (14)—we propose that UVB-primed neutrophils adopt functionally distinct yet overlapping states that enable local inflammation and systemic dissemination. A subset of neutrophils undergoes terminal NETosis (13) to drive local skin inflammation via the

release of NET-associated cytokines/C3. In parallel, the surviving, non-NETting, CXCR4-expressing neutrophils retain migratory capability, undergo RTM to re-enter the circulation, and are subsequently recruited to the kidneys, where CXCL12 levels are elevated—either following UVB irradiation (35) or intrinsically in various lupus-prone strains, including MRL/*lpr* mice (44). Importantly, these phenotypic states are not mutually exclusive: CXCR4 expression is observed across neutrophils irrespective of NETotic status, and a proportion of $CXCR4^{+}$ cells also exhibit features of NETosis, indicating a continuum of activation rather than a strictly binary fate decision. Once sequestered within the glomerular microenvironment, these primed neutrophils subsequently undergo NETosis, releasing pre-expressed cytokines/C3 with NETs, thereby transducing a cutaneous insult into renal injury.

Genetic deficiency of Cxcr4 impaired UVB-induced neutrophil transmigration from the skin to the kidneys. To definitively investigate the causal link between skin UVB exposure and systemic renal injury, we employed a precise spatiotemporal photoconversion tracking model. By crossing Cxcr4-deficient mice with the photoconvertible reporter *kikGR*-expressing mice, we generated *kikGR;Cxcr4*$^{+/-}$ mice (Fig 6A) that were able to "tag" neutrophils in the skin with violet light and monitor their migration across other organ systems. These mice allowed for precise spatiotemporal *in vivo* tracking of neutrophil migration (49), providing an approach to directly observe the effect of CXCR4 absence on cellular trafficking. Sequential irradiation with both UVB and violet light triggered an increase in photoconverted $kikR^{+}$ neutrophils in the circulation, as detected by flow cytometry (Fig 6B). Critically, Cxcr4 deficiency significantly reduced the number of circulating $kikR^{+}$ neutrophils in *kikGR;Cxcr4*$^{+/-}$ mice compared to their controls (Fig 6B), indicating the crucial role of CXCR4 in neutrophil RTM from UVB-irradiated skin into the circulation.

Importantly, direct histological analysis revealed a significant accumulation of ly6G$^+$ and kikR$^+$ neutrophils within the glomeruli of UVB-irradiated control *kikGR;Cxcr4^{flox}* mice following violet light exposure (Fig 6C,E,F). However, the numbers of accumulated ly6G$^+$ and kikR$^+$ neutrophils in the glomeruli were significantly reduced in the *Cxcr4* deficient *kikGR;Cxcr4$^{+/-}$* mice (Fig 6D,E,F). These data provide direct visual and quantitative evidence that CXCR4 is a causal mediator guiding neutrophil transmigration from a site of skin inflammation to the kidneys. Consequently, the decreased neutrophil transmigration resulted in significantly reduced proteinuria in UVB-irradiated *kikGR;Cxcr4$^{+/-}$* mice compared to controls (Fig 6G). This finding functionally confirms the role of CXCR4-mediated skin-to-kidney neutrophil transmigration which drives acute kidney inflammation and renal injury.

These findings provide mechanistic evidence linking UVB-induced acute skin inflammation to systemic lupus exacerbation. We further elucidated that CXCR4 plays an essential role in guiding the systemic spread of inflammatory signals from localized skin lesions to the kidneys. By identifying CXCR4 as the critical mediator facilitating this skin-to-kidney trafficking, our study suggests a paradigm shift in the therapeutic strategy of photosensitive SLE. Specifically, shifting from broad immunosuppression toward targeted blockade of CXCR4-mediated neutrophil dissemination offers a more precise strategy to uncouple localized skin inflammation from systemic disease exacerbation, thereby interrupting the progression of skin inflammation-triggered internal organ injury in photosensitive SLE.

Pharmacological inhibition of CXCR4 attenuated acute kidney inflammation in UVB-irradiated lupus-prone mice. Building upon our genetic evidence identifying CXCR4 as primary driver of UVB-induced systemic inflammation in non-lupus mice (Fig 6), we further evaluated the translational potential of pharmacological inhibition of CXCR4 by using its selective antagonist IT1t in UVB-irradiated lupus-prone mice (Fig 7A). Crucially,

pharmacological CXCR4 inhibition significantly suppressed the acute renal sequelae of UVB exposure, as evidenced by marked reduction in proteinuria, glomerular hypercellularity, glomerular infiltration of Ly6G-positive neutrophils, and CXCR4-expressing neutrophils in acute kidney inflammation triggered by UVB irradiation (Fig 7B-F). To elucidate the underlying mechanism, we performed *in vitro* transwell migration experiments, which demonstrated that IT1t significantly reduced migratory capacity of neutrophils, thereby validating its role in blocking recruitment to inflamed tissues (Fig 7G).

Our key mechanistic finding is that systemic CXCR4 pharmacological inhibition significantly attenuated acute kidney inflammation in UVB-irradiated MRL/*lpr* mice. This was evidenced by the reductions in proteinuria and glomerular hypercellularity, and most importantly the blockade of neutrophil infiltration into the kidneys. We further define a pathogenic cascade by showing that CXCR4 inhibition not only reduced neutrophil influx but also subsequently ameliorated glomerular accumulation of NETs, and NET-associated inflammatory mediators, including IFNα, IFNγ, IL-17A, and C3 (Fig 7H-M), compared to control MRL/*lpr* mice receiving normal saline. Furthermore, our findings demonstrate a novel pathogenic link between UVB exposure and renal damage, highlighting that CXCR4-mediated neutrophil recruitment drives acute lupus kidney inflammation via the induction of NETosis and the release NET-associated inflammatory mediators.

In addition, CXCR4 inhibition also attenuated dermal, but not epidermal (Suppl Fig 3A), skin thickness and reduced nucleated cell counts in the skin (Suppl Fig 3B-D). This involved a significant decrease in the infiltration of Ly6G neutrophils, NET formation, and NET-associated IFNα and IL-17A in the skin of UVB-irradiated mice treated with IT1t (Suppl Fig 3E,G,H,J). However, no significant differences were observed in CXCR4-expressing neutrophils, NET-associated IFNγ and C3 in the skin between IT1t-treated mice and control mice that received normal saline administration (Suppl Fig 3F,I,K). The efficacy of CXCR4

inhibition—achieved via repeated systemic administration of IT1t—underscores a fundamental role for CXCR4 in coordinating systemic inflammatory responses to UVB. These findings align with previous reports demonstrating that CXCR4 inhibition attenuates sunlight-induced skin cancer by preventing the infiltration of mast cells into the skin (50).

Collectively, our findings elucidate a novel pathogenic mechanism that helps us understand UVB-induced systemic disease flares in photosensitive lupus. We demonstrate that this process is governed by the CXCR4-dependent recruitment of neutrophils, which undergo NETosis to release NET-associated proinflammatory cytokines and C3 within both local skin and distant kidneys. By establishing this causal link, our work identifies nuclear envelope regulation and the CXCR4 pathway as robust therapeutic targets. These specific, druggable pathways offer a novel framework for uncoupling environmental triggers from end-organ damage, providing a high-precision strategy to mitigate acute systemic inflammation in photosensitive lupus.

DISCUSSION

Sunlight overexposure exacerbates lupus by inducing localized skin inflammation and promoting systemic inflammation in various distant organs, particularly kidneys, in both humans and lupus-prone mice (5-8). Our study elucidates a novel pathogenic mechanism underlying UVB-triggered lupus exacerbation, identifying a critical pathway that links localized skin inflammation to distant kidney injury. Using initially asymptomatic, young female lupus-prone mice, we demonstrated that infiltrating neutrophils and their released NETs carry proinflammatory cytokines and cytotoxic complement C3 in both the skin and kidneys, driving inflammation in these organs and the development of proteinuria.

While neutrophil NETosis is a recognized contributor to lupus pathogenesis (15, 36, 37), its role in the acute, environmentally triggered phase of the disease has remained unclear.

These findings provide direct *in vivo* evidence identifying neutrophil NETosis as a key mediator of UVB-induced acute inflammation in both the skin and kidneys. We demonstrate that NETs decorated with pro-inflammatory cytokines (IFNα, IFNγ, IL-17A) and C3 are deposited in both organs, and that their glomerular levels strongly correlate with the severity of kidney injury, specifically proteinuria. In UVB-irradiated lupus-prone mice, non-NETting neutrophils may secrete proinflammatory cytokines and C3 into the extracellular space, however, these cytokines and C3 are often quickly diffused into the systemic circulation and diluted by the bloodstream (14). In contrast, neutrophil NETs serve as physical scaffolds that sequester and present high concentrations of proinflammatory cytokines and cytotoxic C3 (14) within the skin and kidneys. These NET-associated cytokines and C3 not only drive further recruitment of leukocytes but also exacerbate inflammation and tissue injury, particularly proteinuria. This positions NETs and their associated cytokines and C3 not merely as biomarkers but as potent pathogenic effectors that drive autoimmune inflammation and tissue damage in lupus, establishing a self-amplifying cycle—a process potentially exacerbated by the ability of NETotic neutrophils and their remnants to trigger secondary NETosis in naive neutrophils *in vitro* (29) and *in vivo* (30). Our findings thus extend the previously well-documented pathogenic roles of NETosis in chronic CLE, SLE, lupus nephritis (15-18), and UVB-induced skin inflammation models (13,14) to its roles in acute systemic responses to UVB.

Recent mechanistic insights identify nuclear chromatin decondensation and nuclear envelope rupture as decisive cellular events required for nuclear chromatin release and NET formation (37,51). Historically, nuclear chromatin decondensation via peptidyl-arginine deaminase 4 (PAD4)-mediated histone citrullination has been the primary focus of NETosis research (37,51). Although early pharmacological studies suggested PAD4 inhibition could attenuate spontaneous lupus skin and kidney inflammation in aged lupus-prone mice (15),

subsequent genetic and pharmacological studies with PAD4-targeted approaches failed to protect against the development of systemic lupus and lupus skin inflammation in lupus-prone mice, suggesting PAD4-independent pathways (38). Additionally, Pad4 genetic deficiency did not show significant protection in a mouse model of arthritis (52). These significant discrepancies underscore a critical gap in our mechanistic understanding of NETosis and highlight the need to target more fundamental, mandatory steps in the process of NET formation.

Beyond chromatin decondensation, nuclear envelope rupture is a critical structural step facilitating nuclear chromatin release and NET formation. As the primary physical barrier sequestering nuclear chromatin, the nuclear envelope relies on the structural integrity of the nuclear lamina, which is composed of lamin A/C and B (37,51). Although neutrophil elastase is a potent proteolytic enzyme and is involved in NET formation (40), there is no evidence identifying lamins as direct substrates of neutrophil elastase (53). Interestingly, we recently identified that nuclear envelope rupture and NET formation are driven by PKCα-mediated phosphorylation and subsequent disassembly of nuclear lamin B, rather than proteolytic cleavage (13,14,37). This finding shifts the therapeutic focus toward regulating this phosphorylation-dependent nuclear envelope rupture, thereby preventing the release of nuclear chromatin and NET formation.

To test the therapeutic potential of targeting nuclear envelope rupture *in vivo*, we investigated the effects of *Pkcα* genetic deletion on NETosis and inflammation in the skin and kidney of lupus-prone MRL/*lpr* mice. We generated MRL/*lpr;Pkcα*$^{-/-}$ mice by backcrossing the *Pkcα* deficiency onto the MRL/*lpr* background for over ten generations to ensure genetic purity. Notably, this genetic intervention effectively suppressed NETosis by preserving nuclear envelope integrity, which significantly ameliorated skin and kidney inflammation following UVB irradiation in MRL/*lpr;Pkcα*$^{-/-}$ mice compared to control MRL/*lpr* mice. Mechanistically,

these findings are particularly significant as UVB triggers PAF production in the skin (31), a lipid mediator known to prime neutrophils (54) and induce PKCα activation (32). This signaling cascade, in turn, drives the nuclear envelope rupture that is structurally required for NET formation in UVB-irradiated mice (13). To the best of our knowledge, our findings provide the first mechanistic evidence supporting the novel concept that nuclear envelope regulation represents a viable strategy to mitigate NETosis-driven pathology in lupus. They further highlight NETosis as an important therapeutic target in acute flares in photosensitive lupus, and introduce nuclear envelope regulation as a potential strategy for lupus treatment.

A skin-kidney connection in the pathological context has long been suggested by clinical observations, such as proteinuria following skin thermal burns (55), emerging evidence suggests activated neutrophils contribute to this process, potentially through the release of neutrophil gelatinase-associated lipocalin (34). This link is supported by a recent mouse study where a single high-dose treatment with UVB caused transient proteinuria and demonstrated the transmigration of neutrophils from the inflamed skin to the kidneys (35). Collectively, these studies across various settings have highlighted a critical role for neutrophils in linking acute skin inflammation to subsequent kidney injury (34,35), indicating dermal-renal communications across different scenarios. Building on this paradigm, our study provides direct correlative evidence that strengthens this link in the context of lupus. We found that the severity of skin inflammation (measured by nucleated cell count and neutrophil infiltration) strongly correlated with the renal injury and proteinuria. This coordinated exacerbation strongly suggests a systemic connection between the two organs rather than two independent disease processes, positioning neutrophils as a crucial mediator for this skin-renal communication.

To address the mechanisms of inter-organ communication, we found that UVB irradiation primed skin-infiltrating neutrophils to express transmigratory CXCR4. This receptor acts as a potent mediator for transmigration of various cell types, including

neutrophils, and facilitates their trafficking between different organs (41,42). This finding provides a crucial mechanistic link to the CXCR4/CXCL12 axis, a pathway increasingly recognized for its role in the systemic progression of lupus (43-48). The recruitment of CXCR4-expressing immune cells, including neutrophils, into the kidneys, is driven by the localized expression of the ligand CXCL12, which is highly expressed in the kidneys of both lupus nephritis patients and lupus-prone mice (43-45,48). Furthermore, CXCR4-expressing immune cells are recruited to the kidneys with CXCL12 expression in mice with ischemic-renal injury (56) and with UVB-induced acute kidney injury (35). These observations identify UVB-induced CXCR4 upregulation as a functional checkpoint that converts a localized skin environmental insult into a systemic, organ-targeting threat. Our findings thus underscore the critical role of immune cell infiltration, particularly neutrophils, in initiating lupus kidney inflammation and driving the development of lupus nephritis (57).

A previously unrecognized finding of this study is the co-expression of CXCR4, pro-inflammatory cytokines (IFNα, IFNγ, IL-17A), and C3 within infiltrating neutrophils and their associated NETs in both the skin and kidneys of UVB-irradiated lupus-prone mice. Mechanistically, UVB—either directly or indirectly through PAF (54)—primes skin-infiltrating neutrophils to concurrently upregulate the transmigratory CXCR4 and pathogenic proinflammatory mediators, positioning neutrophils as a critical cellular bridge linking localized skin inflammation to systemic kidney injury. Consistent with prior *in vitro* and *in vivo* observations (39,40,58), as well as our recent work in UVB-irradiated mice (14), only a portion of neutrophils undergoes NETosis. In this study, we found that NETotic neutrophils in the skin release their pre-expressed proinflammatory cytokines and C3 to fuel local skin inflammation. On the other hand, the surviving, non-NETting neutrophils utilize upregulated CXCR4 for RTM from the inflamed skin back into the circulation (41,42), and are subsequently recruited to the kidneys of UVB-irradiated MRL/*lpr* mice, a process likely driven by renal

CXCL12 expression observed both intrinsically in various lupus-prone strains and in UVB-irradiated WT mice (35,44).

Once sequestered in the kidneys, these primed neutrophils subsequently undergo NETosis to release their pre-expressed cytokines and C3, thereby driving acute local inflammation, kidney injury, and proteinuria in UVB-triggered systemic exacerbation. While most studies report that NETosis typically occurs within 2-3 hours of stimulation (13,14,37), the literature also supports delayed NETosis occurring 4-6 hours after UVB irradiation (13) and even up to 24-48 hours following stimulation with PMA, LPS, or G-CSF (59). This temporal flexibility is further evidenced by a second wave of NETosis in the liver occurring several days after LPS injection, triggered by vascular NET remnants from the initial wave (30). This temporal framework explains our current findings, in which primed, non-NETting neutrophils migrate from the skin to the kidneys, where they subsequently undergo NETosis to release their pre-expressed cytokines and C3, thereby driving the systemic lupus exacerbation in UVB-irradiated mice.

Utilizing the unique spatiotemporal *in vivo* tracking technique inherent in the *kikGR;Cxcr4*$^{+/-}$ mouse model, our study definitively delineates the causal role of CXCR4 in orchestrating the systemic propagation of inflammation via neutrophil RTM (41,42). Our results provide direct *in vivo* evidence that CXCR4 governs the egress of activated neutrophils from the site of primary skin inflammation (UVB-irradiated skin) back into the circulation, a process essential for the subsequent pathological sequestration of neutrophils in distant organs, specifically the kidney glomeruli. Mechanistically, the significantly decreased numbers of kikR^{+} neutrophils observed in both the circulation and renal compartments of *kikGR;Cxcr4*$^{+/-}$ mice, compared to *kikGR;Cxcr4*^{flox} controls, unequivocally demonstrates that Cxcr4 deficiency profoundly disrupts neutrophil mobilization and redistribution. This finding advances the emerging paradigm that demonstrates the involvement of the CXCR4-CXCL12 axis in

neutrophil re-entry into the circulation and re-deposition in the kidneys. Our genetic deficiency approach thus positions CXCR4 as the key molecular determinant controlling access to this systemic circuit. While focused on UVB-induced acute effects, our findings are in line with previous clinical and animal studies that the CXCR4-CXCL12 axis contributes broadly to SLE pathogenesis, including increased CXCR4 expression on immune cells and elevated CXCL12 expression in the kidneys in both SLE patients and lupus-prone mouse strains (43-46,48).

Our study indicates localized skin inflammation from a self-limiting event into a critical driver of distant organ injury by identifying a non-redundant role of CXCR4 in orchestrating neutrophil RTM in photosensitive lupus. Through definitive genetic loss-of-function studies, we demonstrate that Cxcr4 deficiency creates a functional blockage that prevents activated neutrophils from re-entering the circulation, thereby depleting the systemic pool of primed pathogenic effectors. This establishes a clear causal chain from cutaneous UVB exposure to renal neutrophil accumulation, subsequent NET formation, and proteinuria. We further translate this mechanistic insight into a potential therapeutic strategy using the selective CXCR4 antagonist IT1t, which provided significant therapeutic benefits in UVB-irradiated lupus-prone mice. Interestingly, IT1t also reduced dermal skin thickness and neutrophil infiltration and NET deposition specifically within the dermis, without affecting the epidermis. This compartment-specific effect confirms that CXCR4 signaling is essential for immune cell migration into the skin dermis, consistent with prior reports (50). While previous studies identified CXCR4 as a negative regulator of TLR7-mediated IFN-I signaling in plasmacytoid dendritic cells (60), our work expands this framework by showing that CXCR4 inhibition also blocks neutrophil transmigration to the kidneys.

Ultimately, these findings support an integrated two-step model of disease propagation: UVB induces skin-infiltrating neutrophil NETosis and promotes the transmigration of non-NETting neutrophils from the skin to the kidneys, where they subsequently undergo NETosis

to propagate kidney inflammation and injury. By elucidating the requirements for PKCα-driven nuclear envelope rupture during NET release and CXCR4-mediated neutrophil trafficking, this study suggests a shift in therapeutic strategy toward the targeted inhibition of these non-redundant steps. Specifically, PKCα inhibition to control terminal NETosis and CXCR4 blockade to prevent neutrophil transmigration offer a high-precision strategy to neutralize systemic lupus inflammation and protect against distant end-organ damage from cutaneous environmental triggers in photosensitive SLE.

METHODS

Sex as a biological variable. Given the profound female bias in human lupus (~90% patients) and the accelerated disease kinetics in female MRL/*lpr* lupus-prone mice, all experiments within the lupus context exclusively utilized female mice. However, for experiments studying *in vivo* neutrophil transmigration using Cxcr4 deficient strains on a non-lupus background, both sexes were included.

Mice. MRL/*lpr* lupus-prone mice and *Pkcα*-deficient mice (B6;129-*Prkca* ^{tm1Jmk}/J mice, JAX #009068) (61), along with their corresponding littermate controls, were purchased from the Jackson Laboratory, and housed in a pathogen-free environment, and provided food and water *ad libitum*. To generate the MRL/*lpr;Pkcα*$^{-/-}$, lupus-prone mice with Pkcα deficiency, Pkcα$^{-/-}$ mice were backcrossed onto the MRL/*lpr* genetic background for at least 10 generations. For *in vivo* spatiotemporal tracking of neutrophil transmigration from the skin to the kidneys, we generated *kikGR;Cxcr4*$^{+/-}$ (Kikume Green-Red) mice, as homozygous *Cxcr4* deficiency results in perinatal lethality. Briefly, *Cxcr4*^{flox} mice (JAX, #008767) were crossed with *CMV-Cre* mice (JAX, #006054) to create *Cxcr4*-deficient mice, which were then crossed with *kikGR*-expressing mice (JAX, #035393) (49). This model enabled the visualization of neutrophil

trafficking via kikGR fluorescence, with *kikGR;Cxcr4*^{flox} mice serving as controls. All animal experiments were approved by the Institutional Animal Care and Use Committee (IACUC) of the Philadelphia VA Medical Center.

UVB exposure and sample harvest. The dorsal skins of 8-week-old, asymptomatic young female MRL/*lpr* or MRL/*lpr;Pkcα*$^{-/-}$ mice were subjected to UVB irradiation (150 mJ/cm^2/day) or not (sham control) for 5 consecutive days under anesthetization, as previously described (13, 14,62). In separate pharmacological studies, eight-week-old asymptomatic female MRL/*lpr* mice received daily intraperitoneal injections of either the CXCR4 selective antagonist IT1t (10 mg/kg/day) or a sterile normal saline (vehicle control). Pharmacological treatment began one day prior to the 5-day UVB regimen and continued for 6 consecutive days. Each experimental cohort consisted of 5-10 mice.

To enable the spatiotemporal tracking of neutrophils migration *in vivo* from the skin and their infiltration to the kidneys, *kikGR;Cxcr4*$^{+/-}$ and *kikGR;Cxcr4*^{flox} control mice were subjected to a sequential UVB irradiation and violet light photoconversion over five consecutive days. Each day, the shaved dorsal skin was first exposed to UVB irradiation (150 mJ/cm^2/day (13,14). Then, the kikGR green protein expressing in the infiltrating neutrophils was converted to red fluorescence by applying violet light (405 nm) as described (35). The violet-blue light was supplied by a 50 W LED lamp (0.37 numerical aperture fiber, Mightex) at 100 mW, illuminating round skin spots (~2cm in diameter) on the marked area of UVB-irradiated dorsal skin for approximately 15 min per exposure. This sequential exposure converts the kikGR protein from green to red fluorescence, enabling the *in vivo* spatiotemporal tracking of UVB-activated neutrophils as they migrate from the skin to the kidneys.

One day after the last UVB exposure, all mice were anesthetized and the systemic circulation perfused with EDTA-PBS (50 units/ml) via left-sided cardiac puncture (63). Then

the perfused kidneys and dorsal skin were harvested for following experiments. For histologic studies, the skin or kidney tissues were fixed in 4% paraformaldehyde (PFA) for 24h before paraffin-embedded sectioning to 5 μm thick sections for all mice (13, 14). Proteinuria score was measured for all mice before sacrifice using Chemstrip 2GP (Roche, Indianapolis, IN). A scale of 0–3 was used to correspond to the following total urinary protein levels: 0 (negative), 5–20 mg/dL (trace), 30 mg/dL (+), 100 mg/dL (++), and 500 mg/dL (+++).

Cell Culture and Treatment. Mouse bone marrow (BM) neutrophils from the *femur* and *tibia* BM of MRL/*lpr* mice were isolated as described in our previous publications (13,14), and were purified with a neutrophil isolation kit (Miltenyi Biotec). All of the above primary mouse neutrophils were treated without or with 5 or10 μM PAF, or irradiated without or with UVB at 30-60 mJ/cm^2, and cultured for 20h (13,14) for analysis of neutrophil expression of IFNγ and IL-17A cytokines, complement C3 (C3c), or CXCR4. For induction of IFNα in neutrophils, above neutrophils were co-incubated with purified DNA-NETs that were prepared and isolated as described before (13, 14). Then, neutrophils were fixed with 2% PFA and stored at -20 °C for later analysis.

Flow cytometry analysis. To detect UVB-induced neutrophil expression of CXCR4, IFNα, IFNγ, IL-17A, and C3, primary MRL/*lpr* mouse neutrophils were treated without or with PAF (10 μM PAF) or UVB (60 mJ/cm^2), and incubated for 20h, followed by fixation with 2% PFA. Then these cells were first permeabilized with 0.1% Tween-20 and co-stained by PE-labeled anti-mouse Ly6G, FITC-labeled anti-mouse IFNα, IFNγ, IL-17A, or C3, and APC-labeled anti-mouse CXCR4. Analyses of expressions of CXCR4, and/or cytokines, C3 in neutrophils were based on gated cells that were Ly6G positive cells. Flow cytometry analyses were conducted by FACS Canto, and data were analyzed by Flowjo software as described before (14).

Transmigration Assays. To study the effects of CXCR4-CXCL12 signaling pathway on neutrophil migration in the context of UVB, the transmigration ability of primary neutrophils from MRL/*lpr* mice was examined by using Boyden chamber as previously described (13,14, 44). Primary neutrophils from MRL/*lpr* mice were first stimulated by 10 μM PAF for 20h to induce their CXCR4 expression. To study the effects of CXCR4 inhibitor, neutrophils (4 x 10^5) from MRL/*lpr* mice with PAF pretreatment were treated or not by 10 μM IT1t, a selective CXCR4 antagonist, for 30 min before adding to the upper chamber with 3 μm pore inserts of 24-well trans-well plates, followed by stimulation with CXCL12 (300 ng/ml) in the bottom well for 5h. The pore transmigration ability was expressed as relative transmigration compared to that in control neutrophils of the mice without treatment as described before (14).

Immunohistochemistry analyses of the skin and kidneys. The paraffin-embedded skin or kidney tissue sections of all mice were stained either by hematoxylin and eosin (H&E) or by fluorescent staining as described before (13,14). Infiltration of inflammatory cells in skin of all mice was counted for the nucleated cells in the epidermis, dermis, or fat of the H&E stained skin sections as described in our published works (13,14). The glomerular cellularity, including podocytes, endothelial cells, mesangial cells, and infiltrated cells of the kidney cross sections of all mice, was counted as described before with modifications (64). In fluorescent staining, the neutrophil markers PE-labeled anti-ly6G or Alexa-647-labeled myeloperoxidase (MPO) were used for detection of neutrophils and NETosis in combination with FITC-labeled citH3, and DNA staining with DAPI as described before (13). FITC-labeled anti-mouse antibodies against IFNα, IFNγ, IL-17A, C3, or CXCR4 were used to stain the corresponding molecules in the skin or kidneys. The fluorescently matched isotype control immunoglobulins were used as isotype control staining. Slides were mounted with Gold Antifade Mountant (Invitrogen).

The fluorescent images were analyzed with an Olympus Fluoview 1000 confocal microscope or Leica fluorescent microscope. To analyze images for molecular quantification in IHC analyses, the 2D high resolution fluorescent images from at least 5-6 random non-adjacent areas of dermis per skin section, or 20 random glomeruli per mouse kidney section, were captured with an Olympus confocal or Leica fluorescent microscopes and saved as .tiff files. The images were analyzed with NIH ImageJ software by following step-by-step workflow according to the published protocols (65,66). Quantification of the molecules of interest, i.e. neutrophils, NETs, cytokines, or C3, and CXCR4 were based on an automatic threshold analysis of immunofluorescence images to automatically identify the top brightest structures of each image as described in our published work (13,14).

*Statistical analyses***.** GraphPad Prism 6 was used to perform statistical analysis. Normally distributed data are shown as means ± standard deviations (SD). Comparisons between two groups were conducted with student's T test. Comparisons amongst three or more groups were performed using ANOVA, followed by Student-Newman-Keuls (SNK) test. Pearson's correlation coefficient was used for analyses of a linear association between two variables. Statistical significance was considered at a level of P-value < 0.05.

AUTHOR CONTRIBUTIONS

The research was conducted at the University of Pennsylvania and VAMC in Philadelphia. Liu conceived and designed the study. Lyu, Li, Yi, and Liu performed the laboratory experiments and acquired the experimental data. For the microscopic image analysis, Lyu, Liu, Yi took the images, Lyu and Li conducted further quantification and statistical analysis. Liu and Lyu analyzed and interpreted the data and finalized the paper. Lyu, Li, Zhang, Wei, Werth and Liu were involved in the investigation, preparation and revision of the manuscript. All authors read and approved the final manuscript.

ACKNOWLEDGEMENTS

The authors would like to acknowledge Penn Skin Biology and Diseases Resource-based Center for their skin histology service. The authors would thank Debra A. Pawlowski (animal facility, Philadelphia VA Medical Center) for her kindly help with our animal experiments. This work was supported by Lupus Research Alliance (416805) and NIH R21AI144838 (to MLL), Veterans Affairs Merit Review Award (1I01BX005921) and NIH R01 5R01AR076766 (to VPW), NIH 1R41AR082749-01 (to Werth, Liu).

FIGURE LEGENDS

Figure 1. UVB irradiation triggered acute skin and kidney inflammation, neutrophil infiltration and NET formation in young female lupus-prone mice. A. Asymptomatic young female MRL/*lpr* mice were irradiated by UVB (150 mJ/cm^2/day) for 5 days, with urine, skin and kidney samples collected on day 6. **B-E**. Representative H&E images (B) and summary data showing increased epidermal (C), dermal (D) skin thickness, and inflammatory cell infiltration (E, nucleated cell count) in the skin of MRL/*lpr* mice without (sham) or with UVB irradiation. **F-H**. Summary of proteinuria scores (F) and glomerular cellularity (H) with representative glomerular H&E images (G) in asymptomatic young female MRL/*lpr* mice without or with UVB irradiation. **I-O**. Summary analysis of skin neutrophils (I), citH3$^+$ NETs (J,K), and NET-associated IFNα, IFNγ, IL-17A, and C3 (L-O) in the skin of MRL/*lpr* mice without or with UVB- irradiation. In panels I-O, neutrophils, NETs and NET-associated IFNα, IFNγ, IL-17A, and C3 in kidney sections from all mice were stained with PE-labeled anti-ly6G, FITC-labeled antibodies against citH3, IFNα, IFNγ, IL-17A, C3, and DAPI for DNA. Yellow arrows indicate neutrophil NETs (K). **P-Q**. Pearson correlations between dermal nucleated cell count (P) or neutrophil infiltration (Q) and proteinuria scores. Scale bars, 100 µm (B,K), and 50 µm (G). Results represent 5 biological replicates per group. Panels C,D-F,H-J,L-O display means ± SD, $P<0.05$ or <0.01 were determined by student's t-test for two-group comparisons.

Figure 2. Neutrophil infiltration and NET formation drives acute kidney inflammation in asymptomatic young female lupus-prone mice with UVB irradiation. A-H. Summary analysis and representative images of neutrophils (A), citH3$^+$ NETs (B-C), and NET-associated IFNα, IFNγ, IL-17A, and C3 (D-H), in the kidneys of MRL/*lpr* mice without or with UVB irradiation. Sections were stained with PE-labeled anti-ly6G, FITC-labeled antibodies against

citH3, IFNα, IFNγ, IL-17A, C3, and DAPI for DNA. In panels B and H, yellow arrows indicate NETs, and light blue arrows indicate intact non-NETting neutrophils. Scale bars, 50 µm. **I-K**. Pearson correlations between renal NETs, NET-associated IFNα and C3 deposition in kidneys and proteinuria scores in combined groups of mice. Results represent 5 biological replicates per group. Panels A,C-G display mean ± SD, P<0.05 or P<0.01 were determined by student's t-test.

Figure 3. Controlling NETosis via nuclear envelope regulation reduced UVB-induced lupus skin inflammation in MRL/*lpr;Pkcα*$^{-/-}$ mice. A. Asymptomatic female MRL/*lpr* and MRL/*lpr;Pkcα*$^{-/-}$ mice received UVB irradiation (150 mJ/cm^2/day, 5 days), then urine, skin and kidney samples were harvested on day 6 following cardiac perfusion. **B-D**. Histological quantification of skin thickness of epidermis (B), dermis (C), and proinflammatory cell infiltration (D, nucleated cells) in MRL/*lpr* vs MRL/*lpr;Pkcα*$^{-/-}$ mice without or with UVB irradiation. **E-K**. Analyses of skin neutrophils (E), and NET-associated IFNα (F-H), IFNγ, IL-17A, and C3 (I-K). Skin sections were stained with PE-labeled anti-ly6G, FITC-labeled antibodies against IFNα, IFNγ, IL-17A, or C3, and DAPI for DNA. Scale bars, 100 µm. Data represent 5-10 biological replicates. Panels B-F and I-K display mean ± SD; P<0.01 or P<0.001 by one-way ANOVA with SNK post-hoc test.

Figure 4. Inhibiting NETosis through nuclear envelope regulation attenuated acute kidney inflammation in UVB-irradiated MRL/*lpr;Pkcα*$^{-/-}$ mice. A-C. Quantification of proteinuria scores (A) or glomerular cellularity (B), with representative glomerular images (C) for MRL/*lpr* vs MRL/*lpr;Pkcα*$^{-/-}$ mice without or with UVB irradiation. **D-I**. Analysis of glomerular neutrophils (D), and NET-associated IFNα (E,F), IFNγ, IL-17A, C3 (G-I) in MRL/*lpr* vs MRL/*lpr;Pkcα*$^{-/-}$ mice without or with UVB irradiation. Kidney sections were

stained with PE-labeled anti-ly6G, FITC-labeled antibodies against IFNα, IFNγ, IL-17A, or C3, and DAPI for DNA. Scale bars, 50 µm. Results represent 5-10 biological replicates. Panels A,B,D,F-I display mean ± SD; P<0.05, P<0.01, and P<0.001 by one-way ANOVA with SNK post-hoc test.

Figure 5. UVB-induced CXCR4 upregulation and co-expression with cytokines and C3 in primary neutrophils from lupus-prone mice. A-D. Immunofluorescence images and summary analysis of MPO and CXCR4 co-expression and deposition of neutrophil NETs in the inflamed skin and kidneys of UVB-irradiated MRL/*lpr* mice. Skin and kidney sections were stained with Alexa 647-labeled MPO, FITC-labeled antibodies against CXCR4, and DAPI for DNA. **E**,**F**. Flow cytometry histograms of CXCR4 expression in peripheral blood neutrophils from MRL/*lpr* mice without or with UVB irradiation (E,F). Peripheral blood neutrophils were stained with PE-labeled anti-mouse ly6G and APC-labeled rat anti-mouse CXCR4 or APC-labeled rat IgG2b isotype control. **G-O**. Representative histogram and summary analyses of flow cytometry data for primary neutrophils from MRL/*lpr* mice stimulated *in vitro* with PAF (10 µM PAF) or UVB (60 mJ/cm^2) and incubated for 20h. Panels show neutrophil expression of CXCR4 (G), and cytokines IFNα (H,I), IFNγ (J,K), IL-17A (L,M), and C3 (N,O). Cells were stained with PE-labeled anti-mouse ly6G, APC-labeled anti-mouse CXCR4, and FITC-labeled anti-mouse IFNα, IFNγ, IF-17A, or C3. All neutrophils in panels E-O were gated on ly6G$^+$ cells. Data represent 4-6 biological replicates. Panels B,D,F,H-O display means ± SD, P<0.05, P<0.01, P<0.001 determined by student's t-test for two-group comparisons.

Figure 6. Cxcr4 genetic deficiency inpaired neutrophil transmigration from skin to kidneys following UVB irradiation. A. Young *kikGR;Cxcr4*$^{+/-}$ and *kikGR;Cxcr4*^{flox} control mice expressing a photo-convertible reporter were irradiated by UVB (150 mJ/cm^2/day) and

violet light for 5 days, then urine, skin and kidney samples were harvested on day 6. **B**. Flow cytometry analysis of peripheral blood kikR$^+$ neutrophils from *kikGR;Cxcr4^{flox}* and *kikGR;Cxcr4$^{+/-}$* mice without or with UVB and violet light irradiation. Analysis was performed to assess systemic circulation, gating on Ly6G$^+$ cells (PE-labeled anti-mouse ly6G) that had photoconverted from kikG$^+$ to kikR$^+$. **C-F**. Immunofluorescence and summary analysis of photoconverted kikR$^+$ neutrophil infiltration into kidneys. Kidney sections were stained with Pacific Blue labeled anti-mouse ly6G, and Alexa 647-labeled CXCR4. Blue arrows indicate glomeruli with deposition of photoconverted kikR$^+$ neutrophils, while yellow arrows denote deposition of neutrophil NET-like structures in glomeruli. Scale bars, 50 µm. **G**. Quantification of proteinuria scores in control *kikGR;Cxcr4^{flox}* and *kikGR;Cxcr4$^{+/-}$* mice without or with UVB and violet light irradiation. Data represent 6 biological replicates in each group (3 male and 3 female mice). Panels E-G display mean ± SD, $P<0.05$, $P<0.01$, and $P<0.001$ determined by one-way ANOVA with SNK post-hoc test.

Figure 7. Pharmacological CXCR4 inhibition attenuated acute kidney inflammation in lupus-prone mice irradiated by UVB. A. Asymptomatic female MRL/*lpr* mice irradiated by UVB (150 mJ/cm^2/day, 5 days), with intraperitoneal administration of CXCR4 antagonist IT1t (10 mg/kg/day, 6 days) began one day prior to the first session of UVB irradiation Then, urine, skin and kidney samples were harvested on day 6 post cardiac perfusion. **B-F**. Quantification of proteinuria scores (B), glomerular cellularity (C,D), renal Ly6G-neutrophils (E) and CXCR4-expressing neutrophils (F) in UVB-irradiated MRL/*lpr* mice without (control) or with IT1t administration. **G**. Relative migration analysis of mouse neutrophils with CXCR4 expression, induced by 10 µM PAF stimulation for 20h, was conducted using a Boyden chamber. Cells were pretreated without or with IT1t, and then stimulated with CXCL12 at 300 ng/ml. **H-M**. Analyses of glomerular deposition of neutrophil NETs, and NET-associated

IFNα, IFNγ, IL-17A, or C3 in glomeruli of UVB-irradiated MRL/*lpr* mice without (control) or with IT1t pre-administration. Sections (E,F,H-M) were immunostained with PE-labeled anti-ly6G, FITC-labeled antibodies against CXCR4, citH3, IFNα, IFNγ, IL-17A, or C3, and DAPI for DNA. Scale bars, 50 µm (D), and 100 µm (I). Data represent 3-5 biological replicates. Panels B,C,E-H,J-M display means ± SD, $P<0.05$, $P<0.01$ by student's t-test for two-group comparisons.

Figure 1

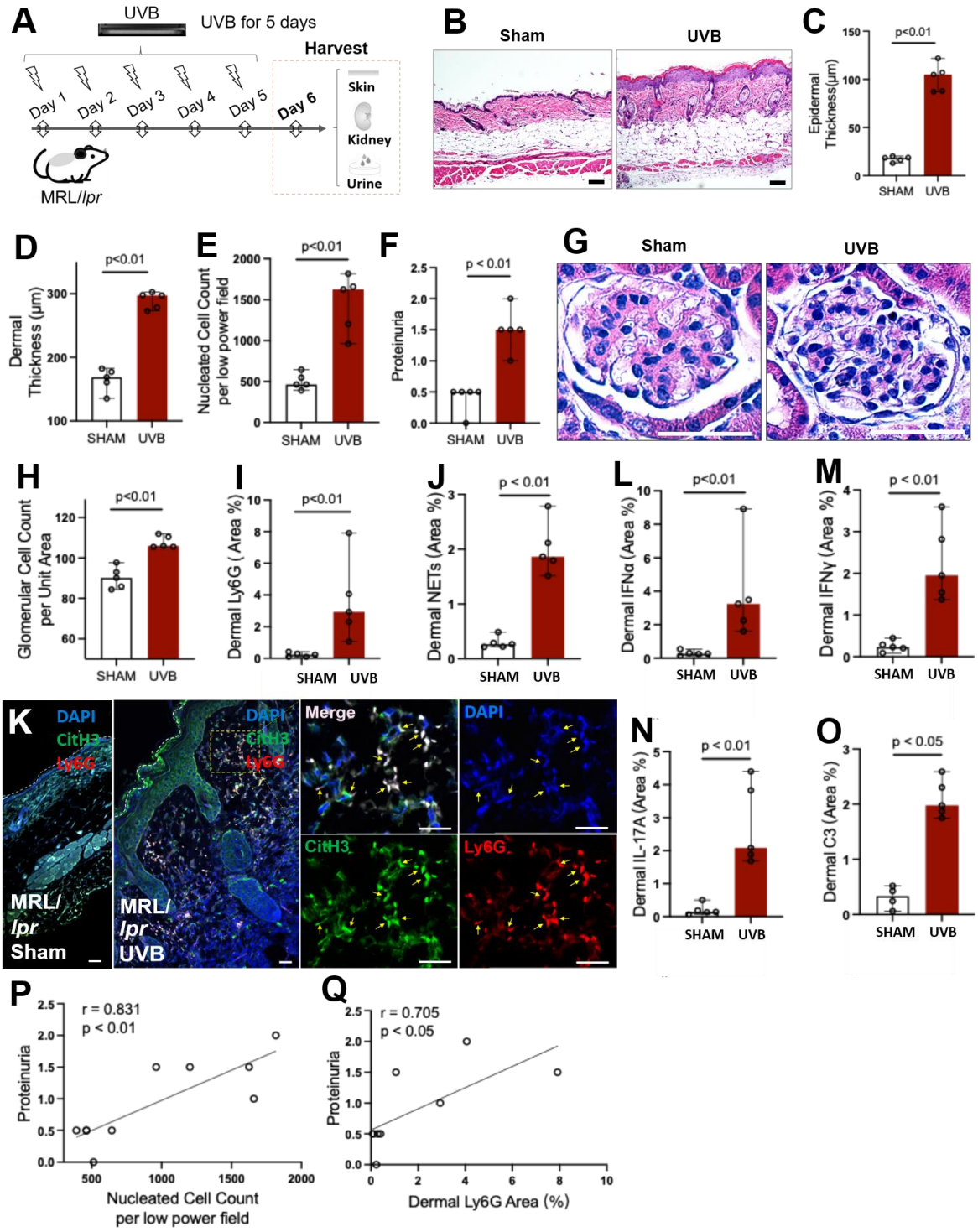
A
UVB
UVB for 5 days
Harvest
Day 1
Day 2
Day 3
Day 4
Day 5
Day 6
Skin
Kidney
Urine
MRL/lpr
B
Sham
UVB
C
p<0.01
Epidermal Thickness(μm)
SHAM
UVB
D
p<0.01
Dermal Thickness (μm)
E
p<0.01
Nucleated Cell Count per low power field
F
p < 0.01
Proteinuria
G
Sham
UVB
H
p<0.01
Glomerular Cell Count per Unit Area
I
p<0.01
Dermal Ly6G (Area %)
J
p < 0.01
Dermal NETs (Area %)
L
p<0.01
Dermal IFNα (Area %)
M
p < 0.01
Dermal IFNγ (Area %)
K
DAPI
CitH3
Ly6G
MRL/lpr Sham
MRL/lpr UVB
Merge
N
p < 0.01
Dermal IL-17A (Area %)
O
p < 0.05
Dermal C3 (Area %)
P
r = 0.831
p < 0.01
Proteinuria
Nucleated Cell Count per low power field
Q
r = 0.705
p < 0.05
Proteinuria
Dermal Ly6G Area (%)

Figure 2.

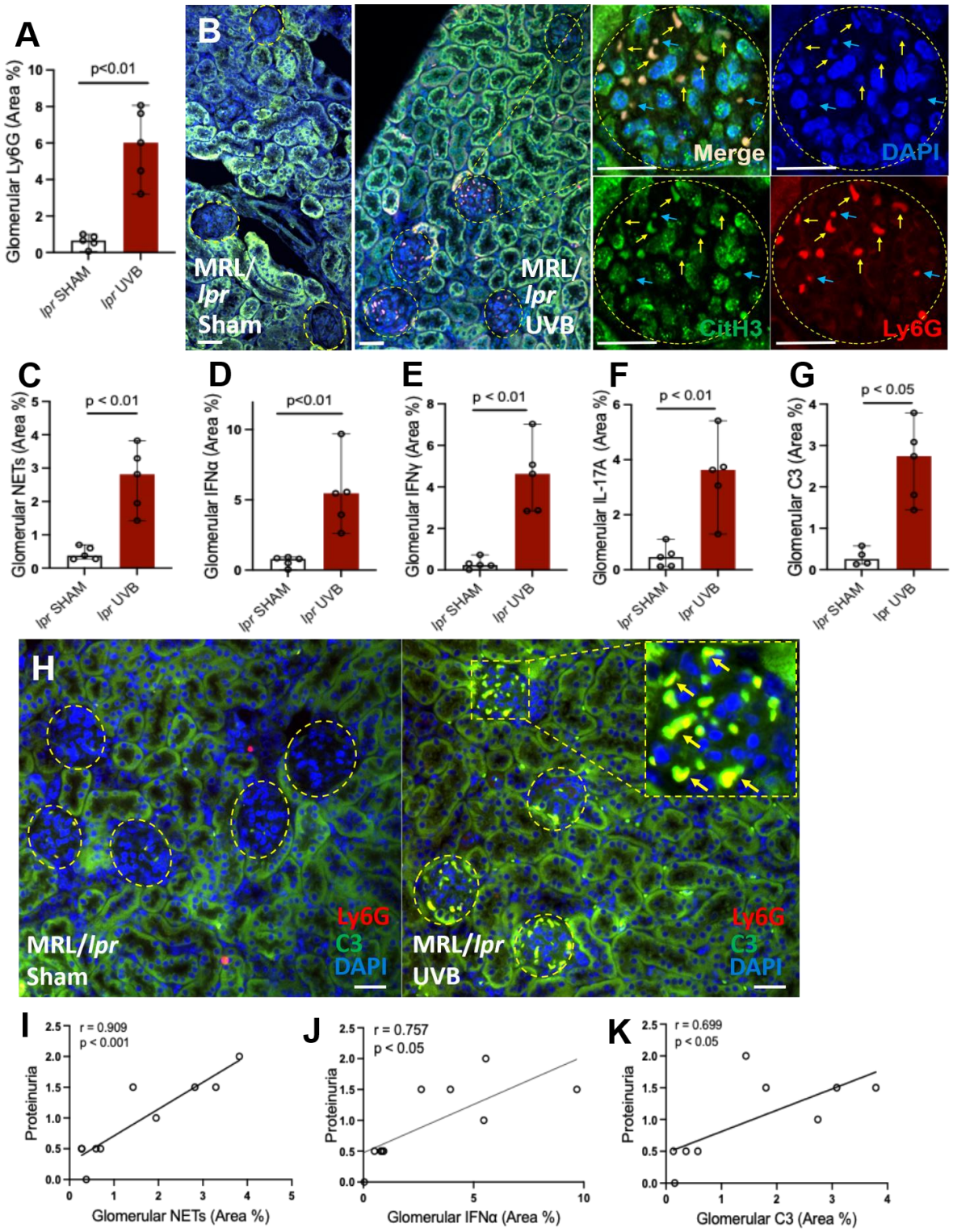
A
p<0.01
Glomerular Ly6G (Area %)
lpr SHAM
lpr UVB
B
MRL/
lpr
Sham
MRL/
lpr
UVB
Merge
DAPI
CitH3
Ly6G
C
p < 0.01
Glomerular NETs (Area %)
D
p<0.01
Glomerular IFNα (Area %)
E
p < 0.01
Glomerular IFNγ (Area %)
F
p < 0.01
Glomerular IL-17A (Area %)
G
p < 0.05
Glomerular C3 (Area %)
H
MRL/lpr
Sham
Ly6G
C3
DAPI
MRL/lpr
UVB
I
r = 0.909
p < 0.001
Proteinuria
Glomerular NETs (Area %)
J
r = 0.757
p < 0.05
Glomerular IFNα (Area %)
K
r = 0.699
p < 0.05
Glomerular C3 (Area %)

Figure 3.

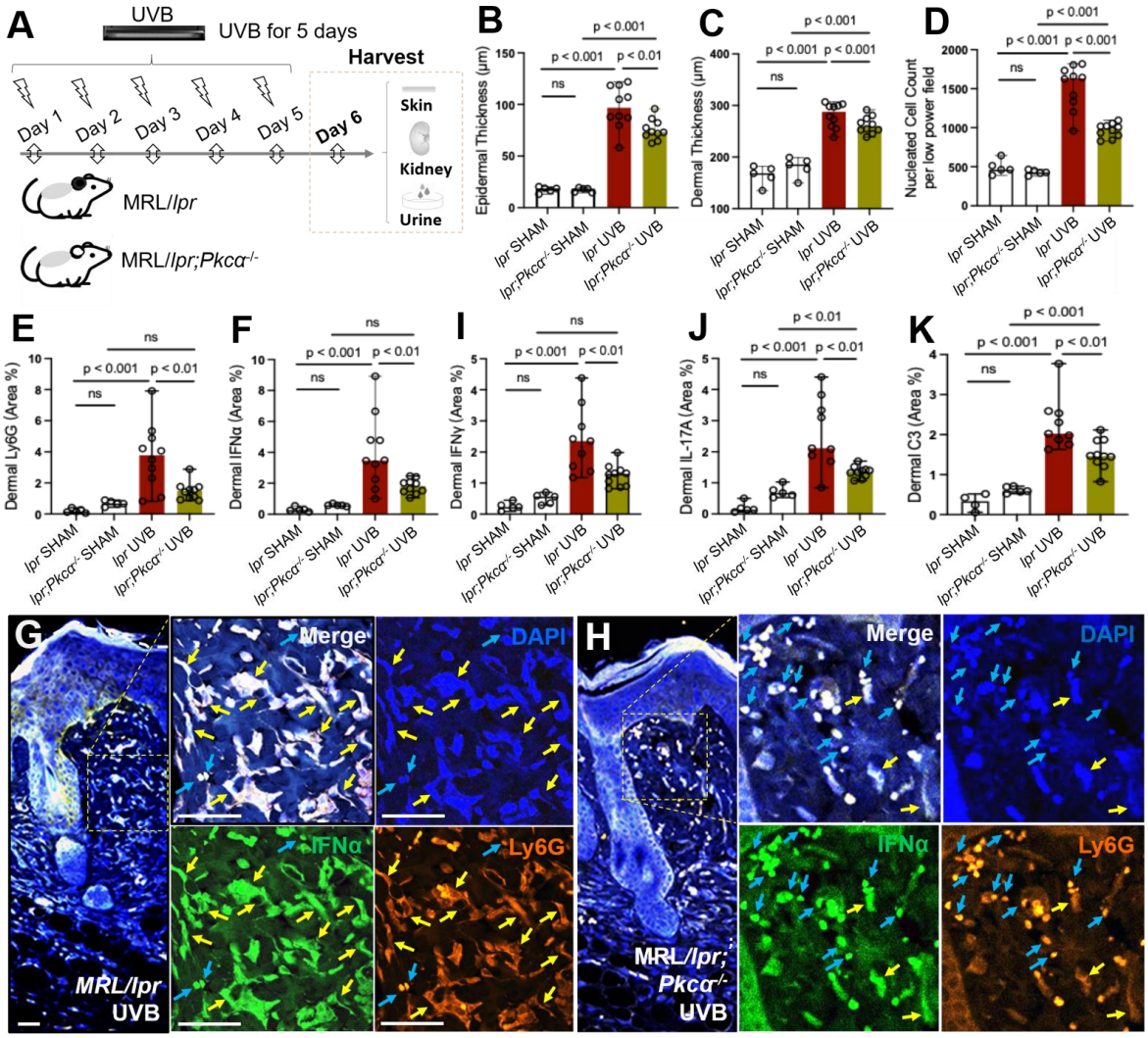
A
UVB
UVB for 5 days
Harvest
Day 1
Day 2
Day 3
Day 4
Day 5
Day 6
Skin
Kidney
Urine
MRL/lpr
MRL/lpr;Pkcα-/-
B
Epidermal Thickness (μm)
C
Dermal Thickness (μm)
D
Nucleated Cell Count per low power field
E
Dermal Ly6G (Area %)
F
Dermal IFNα (Area %)
I
Dermal IFNγ (Area %)
J
Dermal IL-17A (Area %)
K
Dermal C3 (Area %)
lpr SHAM
lpr;Pkcα-/- SHAM
lpr UVB
lpr;Pkcα-/- UVB
ns
p < 0.001
p < 0.01
G
H
Merge
DAPI
IFNα
Ly6G
MRL/lpr UVB
MRL/lpr; Pkcα-/- UVB

Figure 4.

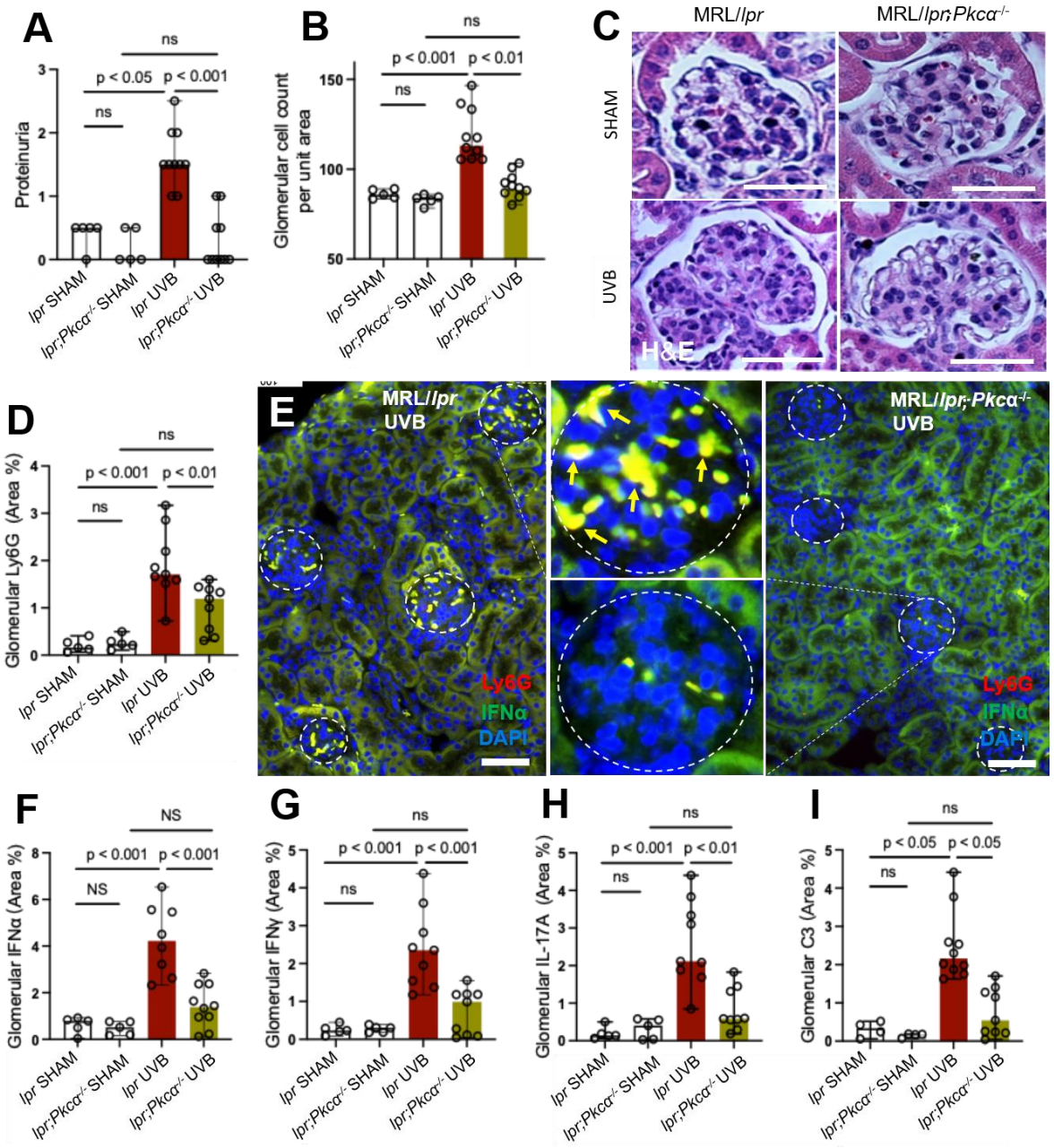
A
Proteinuria
ns
p < 0.05
p < 0.001
ns
lpr SHAM
lpr;Pkcα-/- SHAM
lpr UVB
lpr;Pkcα-/- UVB
B
Glomerular cell count per unit area
ns
p < 0.001
p < 0.01
ns
C
MRL/lpr
MRL/lpr;Pkcα-/-
SHAM
UVB
H&E
D
Glomerular Ly6G (Area %)
ns
p < 0.001
p < 0.01
ns
E
MRL/lpr UVB
MRL/lpr;Pkcα-/- UVB
Ly6G
IFNα
DAPI
F
Glomerular IFNα (Area %)
NS
p < 0.001
p < 0.001
NS
G
Glomerular IFNγ (Area %)
ns
p < 0.001
p < 0.001
ns
H
Glomerular IL-17A (Area %)
ns
p < 0.001
p < 0.01
ns
I
Glomerular C3 (Area %)
ns
p < 0.05
p < 0.05
ns

Figure 5.

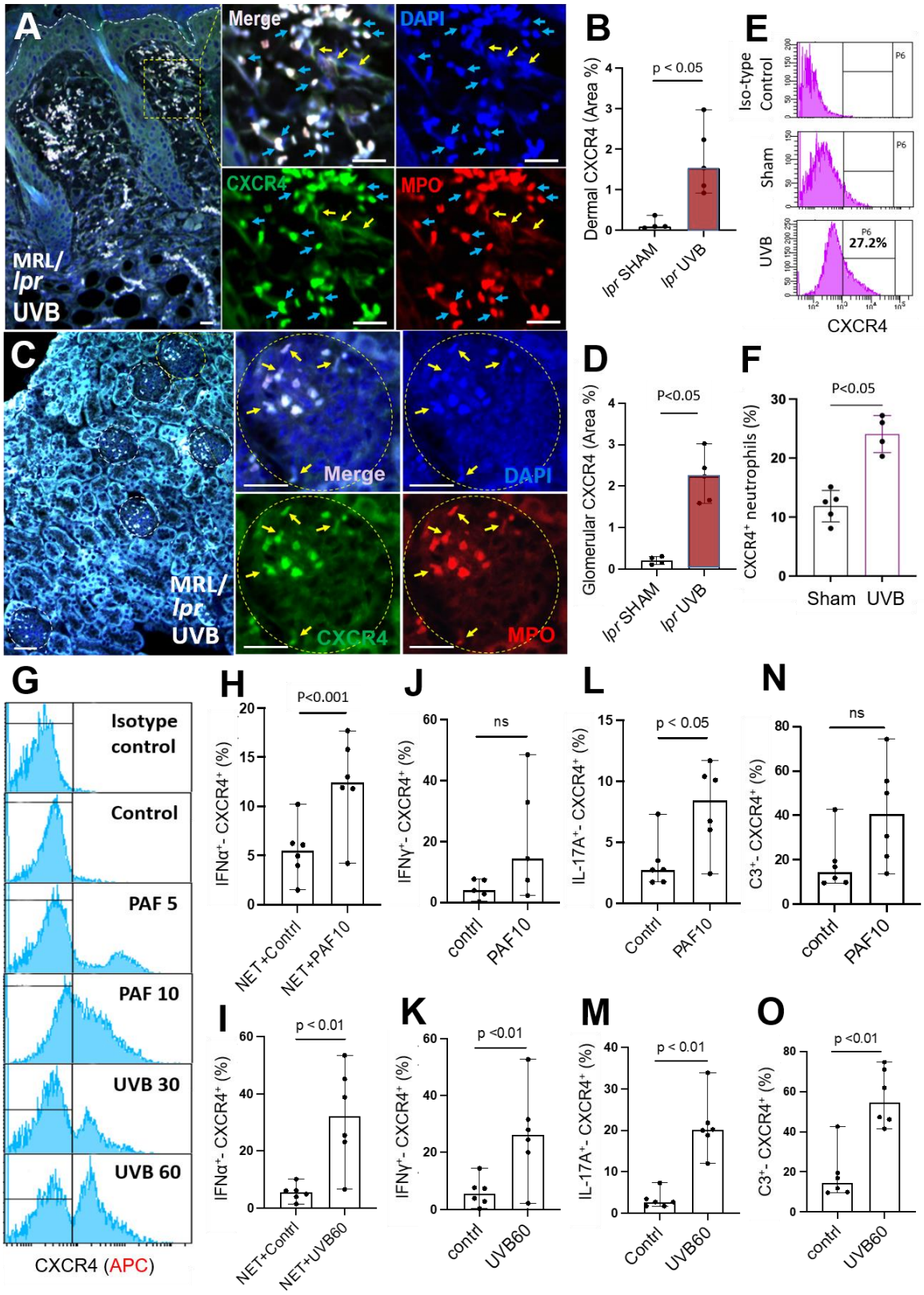
A
Merge
DAPI
CXCR4
MPO
MRL/
lpr
UVB
B
Dermal CXCR4 (Area %)
p < 0.05
lpr SHAM
lpr UVB
E
Iso-type Control
Sham
UVB
P6
27.2%
CXCR4
C
Merge
DAPI
CXCR4
MPO
MRL/
lpr
UVB
D
Glomerular CXCR4 (Area %)
P<0.05
lpr SHAM
lpr UVB
F
CXCR4+ neutrophils (%)
P<0.05
Sham
UVB
G
Isotype control
Control
PAF 5
PAF 10
UVB 30
UVB 60
CXCR4 (APC)
H
IFNα+- CXCR4+ (%)
P<0.001
NET+Contrl
NET+PAF10
J
IFNγ+- CXCR4+ (%)
ns
contrl
PAF10
L
IL-17A+- CXCR4+ (%)
p < 0.05
Contrl
PAF10
N
C3+- CXCR4+ (%)
ns
contrl
PAF10
I
IFNα+- CXCR4+ (%)
p < 0.01
NET+Contrl
NET+UVB60
K
IFNγ+- CXCR4+ (%)
p <0.01
contrl
UVB60
M
IL-17A+- CXCR4+ (%)
p < 0.01
Contrl
UVB60
O
C3+- CXCR4+ (%)
p <0.01
contrl
UVB60

Figure 6.

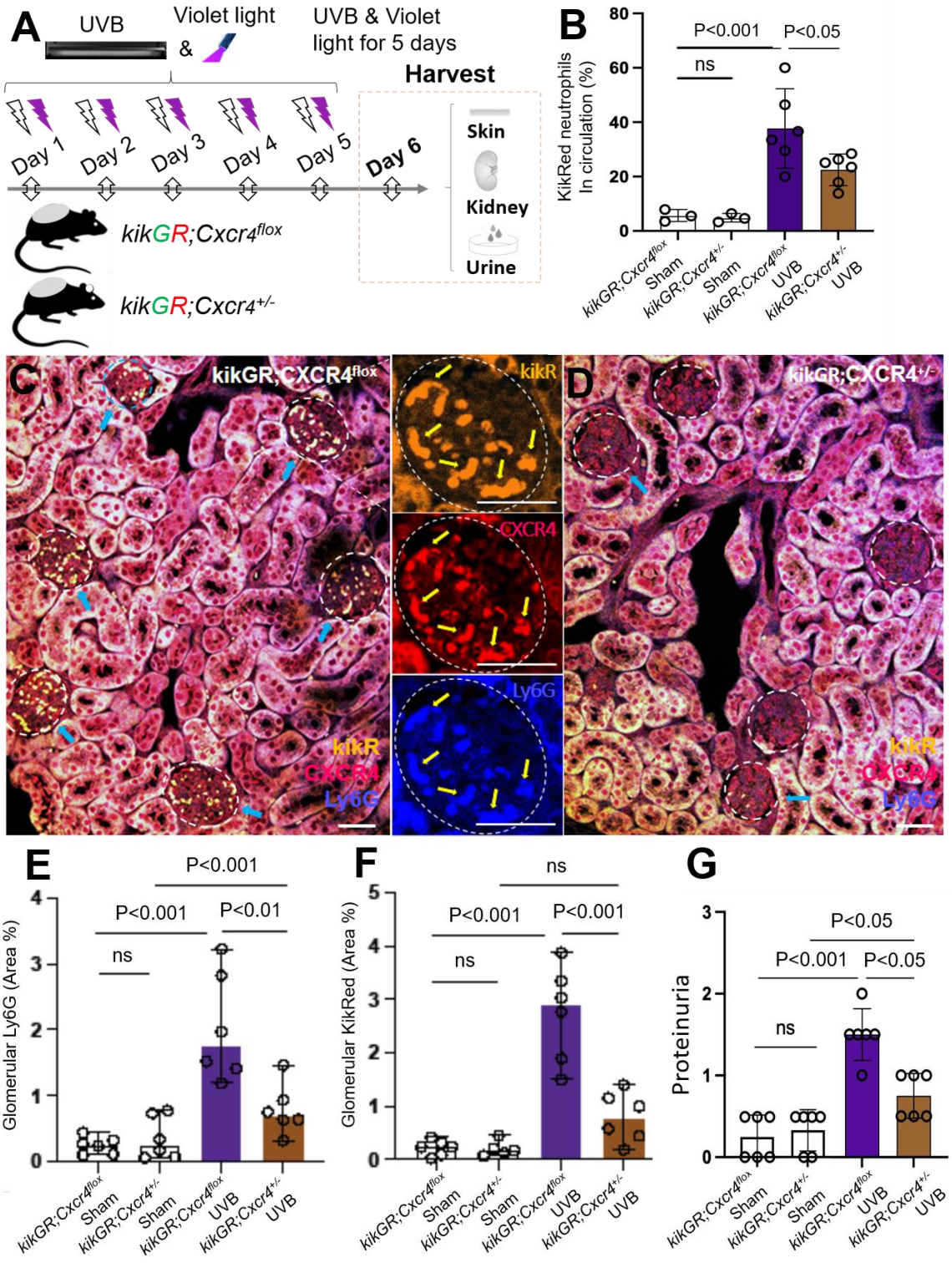
A
UVB
Violet light
&
UVB & Violet light for 5 days
Harvest
Day 1
Day 2
Day 3
Day 4
Day 5
Day 6
Skin
Kidney
Urine
kikGR;Cxcr4flox
kikGR;Cxcr4+/-
B
KikRed neutrophils In circulation (%)
P<0.001
P<0.05
ns
kikGR;Cxcr4flox
Sham
kikGR;Cxcr4+/-
Sham
kikGR;Cxcr4flox
UVB
kikGR;Cxcr4+/-
UVB
C
kikGR;CXCR4flox
kikR
CXCR4
Ly6G
D
kikGR;CXCR4+/-
E
Glomerular Ly6G (Area %)
P<0.001
P<0.001
P<0.01
ns
F
Glomerular KikRed (Area %)
ns
P<0.001
P<0.001
ns
G
Proteinuria
P<0.05
P<0.001
P<0.05
ns

Figure 7.

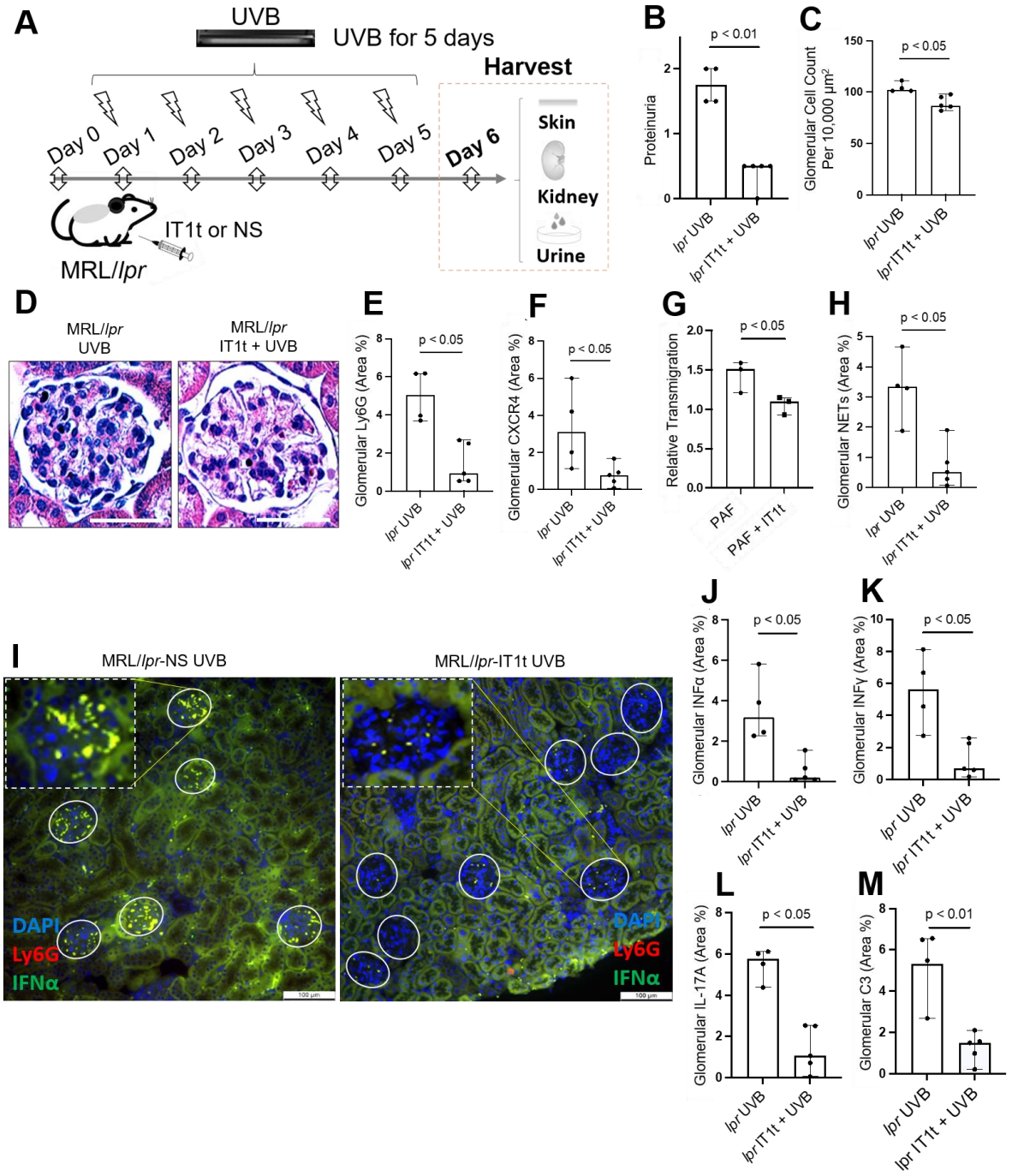
A
UVB
UVB for 5 days
Harvest
Day 0
Day 1
Day 2
Day 3
Day 4
Day 5
Day 6
Skin
Kidney
Urine
IT1t or NS
MRL/lpr
B
p < 0.01
Proteinuria
lpr UVB
lpr IT1t + UVB
C
p < 0.05
Glomerular Cell Count Per 10,000 μm²
D
MRL/lpr UVB
MRL/lpr IT1t + UVB
E
p < 0.05
Glomerular Ly6G (Area %)
F
p < 0.05
Glomerular CXCR4 (Area %)
G
p < 0.05
Relative Transmigration
PAF
PAF + IT1t
H
p < 0.05
Glomerular NETs (Area %)
I
MRL/lpr-NS UVB
MRL/lpr-IT1t UVB
DAPI
Ly6G
IFNα
J
p < 0.05
Glomerular INFα (Area %)
K
p < 0.05
Glomerular INFγ (Area %)
L
p < 0.05
Glomerular IL-17A (Area %)
M
p < 0.01
Glomerular C3 (Area %)

REFERENCES

1. Tsokos GC (2020) Autoimmunity and organ damage in systemic lupus erythematosus. *Nature immunology* 21(6):605-614.
2. Dai C, *et al.* (2014) Genetics of systemic lupus erythematosus: immune responses and end organ resistance to damage. *Current opinion in immunology* 31:87-96.
3. Baer RL & Harber LC (1965) Photobiology of lupus erythematosus. *Archives of dermatology* 92(2):124-128.
4. Foering K, *et al.* (2013) Characterization of clinical photosensitivity in cutaneous lupus erythematosus. *J Am Acad Dermatol* 69(2):205-213.
5. Ansel JC, Mountz J, Steinberg AD, DeFabo E, & Green I (1985) Effects of UV radiation on autoimmune strains of mice: increased mortality and accelerated autoimmunity in BXSB male mice. *The Journal of investigative dermatology* 85(3):181-186.
6. Schmidt E, Tony HP, Brocker EB, & Kneitz C (2007) Sun-induced life-threatening lupus nephritis. *Annals of the New York Academy of Sciences* 1108:35-40.
7. He J, Guo Y, Chen J, Xu J, & Zhu X (2025) Exploring the correlation between UVB sensitivity and SLE activity: Insights into UVB-driven pathogenesis in lupus erythematosus. *Journal of autoimmunity* 153:103393.
8. Sim JH, *et al.* (2021) Immune Cell-Stromal Circuitry in Lupus Photosensitivity. *J Immunol* 206(2):302-309.
9. Chiche L, *et al.* (2012) Seasonal variations of systemic lupus erythematosus flares in southern France. *European journal of internal medicine* 23(3):250-254.
10. Abdelaziz TS, *et al.* (2023) Seasonal variation of lupus nephritis in a cohort of Egyptian patients. *Clin Rheumatol* 42(4):1013-1018.
11. Hawk JL, Murphy GM, & Holden CA (1988) The presence of neutrophils in human cutaneous ultraviolet-B inflammation. *The British journal of dermatology* 118(1):27-30.

12. Han X, *et al.* (2019) PD-1H (VISTA)-mediated suppression of autoimmunity in systemic and cutaneous lupus erythematosus. *Science translational medicine* 11(522).
13. Li Y, *et al.* (2020) Nuclear envelope rupture and NET formation is driven by PKCα-mediated lamin B disassembly. *EMBO reports* 21(e48779).
14. Li M, Lyu X, Liao J, Werth VP, & Liu ML (2022) Rho Kinase regulates neutrophil NET formation that is involved in UVB-induced skin inflammation. *Theranostics* 12(5):2133-2149.
15. Knight JS, *et al.* (2015) Peptidylarginine deiminase inhibition disrupts NET formation and protects against kidney, skin and vascular disease in lupus-prone MRL/lpr mice. *Annals of the rheumatic diseases* 74(12):205365.
16. Safi R, Al-Hage J, Abbas O, Kibbi AG, & Nassar D (2019) Investigating the presence of neutrophil extracellular traps in cutaneous lesions of different subtypes of lupus erythematosus. *Exp Dermatol* 28(11):1348-1352.
17. Westhorpe CL, *et al.* (2017) In Vivo Imaging of Inflamed Glomeruli Reveals Dynamics of Neutrophil Extracellular Trap Formation in Glomerular Capillaries. *The American journal of pathology* 187(2):318-331.
18. Pieterse E, *et al.* (2017) Neutrophil Extracellular Traps Drive Endothelial-to-Mesenchymal Transition. *Arteriosclerosis, thrombosis, and vascular biology* 37(7):1371-1379.
19. Lindau D, *et al.* (2013) TLR9 independent interferon alpha production by neutrophils on NETosis in response to circulating chromatin, a key lupus autoantigen. *Annals of the rheumatic diseases*.
20. Barrat FJ, Crow MK, & Ivashkiv LB (2019) Interferon target-gene expression and epigenomic signatures in health and disease. *Nature immunology* 20(12):1574-1583.

21. Kiefer K, Oropallo MA, Cancro MP, & Marshak-Rothstein A (2012) Role of type I interferons in the activation of autoreactive B cells. *Immunology and cell biology* 90(5):498-504.
22. Gestermann N, *et al.* (2018) Netting Neutrophils Activate Autoreactive B Cells in Lupus. *J Immunol* 200(10):3364-3371.
23. Bertelli R, *et al.* (2021) Neutrophil Extracellular Traps in Systemic Lupus Erythematosus Stimulate IgG2 Production From B Lymphocytes. *Front Med (Lausanne)* 8:635436.
24. Leffler J, *et al.* (2012) Neutrophil extracellular traps that are not degraded in systemic lupus erythematosus activate complement exacerbating the disease. *J Immunol* 188(7):3522-3531.
25. Yuen J, *et al.* (2016) NETosing Neutrophils Activate Complement Both on Their Own NETs and Bacteria via Alternative and Non-alternative Pathways. *Frontiers in immunology* 7:137.
26. Helm KF & Peters MS (1993) Deposition of membrane attack complex in cutaneous lesions of lupus erythematosus. *J Am Acad Dermatol* 28(5 Pt 1):687-691.
27. Zhao Y, Wei W, & Liu ML (2020) Extracellular vesicles and lupus nephritis - New insights into pathophysiology and clinical implications. *Journal of autoimmunity*:102540.
28. Shrestha B, *et al.* (2019) Recombinant Thrombomodulin Suppresses Histone-Induced Neutrophil Extracellular Trap Formation. *Frontiers in immunology* 10:2535.
29. Deng P, *et al.* (2024) Auto-amplification and spatial propagation of neutrophil extracellular traps. *Commun Biol* 7(1):386.
30. Santocki M, Such A, Drab D, Burczyk G, & Kolaczkowska E (2025) NETs persisting in vasculature undergo self-renewal with consequences for subsequent infection: a mouse model study. *Blood* 145(18):2070-2085.

31. Marathe GK, *et al.* (2005) Ultraviolet B radiation generates platelet-activating factor-like phospholipids underlying cutaneous damage. *The Journal of biological chemistry* 280(42):35448-35457.
32. Gay JC & Stitt ES (1988) Platelet-activating factor induces protein kinase activity in the particulate fraction of human neutrophils. *Blood* 71(1):159-165.
33. Yavuz S, *et al.* (2014) Neutrophil gelatinase associated lipocalin as an indicator of acute kidney injury and inflammation in burned children. *Burns* 40(4):648-654.
34. Niculae A, *et al.* (2022) Burn-Induced Acute Kidney Injury-Two-Lane Road: From Molecular to Clinical Aspects. *International journal of molecular sciences* 23(15).
35. Skopelja-Gardner S, *et al.* (2021) Acute skin exposure to ultraviolet light triggers neutrophil-mediated kidney inflammation. *Proceedings of the National Academy of Sciences of the United States of America* 118(3).
36. Mutua V & Gershwin LJ (2020) A Review of Neutrophil Extracellular Traps (NETs) in Disease: Potential Anti-NETs Therapeutics. *Clinical reviews in allergy & immunology*.
37. Singh J, *et al.* (2023) Moonlighting chromatin: when DNA escapes nuclear control. *Cell death and differentiation*:1-15.
38. Gordon RA, *et al.* (2017) Lupus and proliferative nephritis are PAD4 independent in murine models. *JCI insight* 2(10).
39. Sorensen OE & Borregaard N (2016) Neutrophil extracellular traps - the dark side of neutrophils. *The Journal of clinical investigation* 126(5):1612-1620.
40. Yipp BG & Kubes P (2013) NETosis: how vital is it? *Blood* 122(16):2784-2794.
41. De Filippo K & Rankin SM (2018) CXCR4, the master regulator of neutrophil trafficking in homeostasis and disease. *European journal of clinical investigation* 48 Suppl 2:e12949.

42. Wang J, *et al.* (2017) Visualizing the function and fate of neutrophils in sterile injury and repair. *Science (New York, N.Y* 358(6359):111-116.
43. Chong BF & Mohan C (2009) Targeting the CXCR4/CXCL12 axis in systemic lupus erythematosus. *Expert opinion on therapeutic targets* 13(10):1147-1153.
44. Wang A, *et al.* (2009) CXCR4/CXCL12 hyperexpression plays a pivotal role in the pathogenesis of lupus. *J Immunol* 182(7):4448-4458.
45. Wang A, *et al.* (2010) Dysregulated expression of CXCR4/CXCL12 in subsets of patients with systemic lupus erythematosus. *Arthritis and rheumatism* 62(11):3436-3446.
46. Zhao LD, *et al.* (2017) Contribution and underlying mechanisms of CXCR4 overexpression in patients with systemic lupus erythematosus. *Cellular & molecular immunology* 14(10):842-849.
47. Jang SH, *et al.* (2024) Mitochondria Activity and CXCR4 Collaboratively Promote the Differentiation of CD11c(+) B Cells Induced by TLR9 in Lupus. *Immune Netw* 24(4):e25.
48. Hu HM, *et al.* (2025) Dual blockade of DPP-4 and CXCL12/CXCR4 axes synergistically protects podocytes in lupus nephritis. *Frontiers in pharmacology* 16:1732243.
49. Griswold SL, Sajja KC, Jang CW, & Behringer RR (2011) Generation and characterization of iUBC-KikGR photoconvertible transgenic mice for live time-lapse imaging during development. *Genesis* 49(7):591-598.
50. Sarchio SN, *et al.* (2014) Pharmacologically antagonizing the CXCR4-CXCL12 chemokine pathway with AMD3100 inhibits sunlight-induced skin cancer. *The Journal of investigative dermatology* 134(4):1091-1100.
51. Liu ML, Lyu X, & Werth VP (2021) Recent progress in the mechanistic understanding of NET formation in neutrophils. *The FEBS journal* 10.1111/febs.16036.

52. Rohrbach AS, Hemmers S, Arandjelovic S, Corr M, & Mowen KA (2012) PAD4 is not essential for disease in the K/BxN murine autoantibody-mediated model of arthritis. *Arthritis research & therapy* 14(3):R104.

53. Jerke U, *et al.* (2015) Neutrophil serine proteases exert proteolytic activity on endothelial cells. *Kidney international* 88(4):764-775.

54. Metzemaekers M, Gouwy M, & Proost P (2020) Neutrophil chemoattractant receptors in health and disease: double-edged swords. *Cellular & molecular immunology* 17(5):433-450.

55. Jackson SH, Farmer AW, Slater RJ, & Dewolfe MS (1961) The resolution of urinary or serum proteins by chromatography on DEAE cellulose columns with particular reference to urinary proteins after thermal burns. *Can J Biochem Physiol* 39:881-889.

56. Togel F, Isaac J, Hu Z, Weiss K, & Westenfelder C (2005) Renal SDF-1 signals mobilization and homing of CXCR4-positive cells to the kidney after ischemic injury. *Kidney international* 67(5):1772-1784.

57. Jamaly S, Rakaee M, Abdi R, Tsokos GC, & Fenton KA (2021) Interplay of immune and kidney resident cells in the formation of tertiary lymphoid structures in lupus nephritis. *Autoimmunity reviews* 20(12):102980.

58. Phillipson M & Kubes P (2011) The neutrophil in vascular inflammation. *Nature medicine* 17(11):1381-1390.

59. Kolman JP, *et al.* (2022) NET Release of Long-Term Surviving Neutrophils. *Frontiers in immunology* 13:815412.

60. Smith N, *et al.* (2019) Control of TLR7-mediated type I IFN signaling in pDCs through CXCR4 engagement-A new target for lupus treatment. *Sci Adv* 5(7):eaav9019.

61. Braz JC, *et al.* (2004) PKC-alpha regulates cardiac contractility and propensity toward heart failure. *Nature medicine* 10(3):248-254.

62. Li Y, Travers JB, Werth VP, & Liu ML (2018) PKCα deficiency protected mice from UVB induced-Skin Inflammation through attenuation of neutrophil NETosis. *Arthritis Rheumatol* 70(suppl 9).

63. Zhao J, *et al.* (2013) P2X7 blockade attenuates murine lupus nephritis by inhibiting activation of the NLRP3/ASC/caspase 1 pathway. *Arthritis and rheumatism* 65(12):3176-3185.

64. Zhang PL, Herrera GA, & Liu B (2020) Monoclonal glomerulopathy with features of cryoglobulinemic glomerulopathy in murine multiple myeloma model. *Ultrastruct Pathol* 44(4-6):387-394.

65. Guirado R, Carceller H, Castillo-Gomez E, Castren E, & Nacher J (2018) Automated analysis of images for molecular quantification in immunohistochemistry. *Heliyon* 4(6):e00669.

66. Rebollo E, Boix-Fabres J, & Arbones ML (2019) Automated Macro Approach to Quantify Synapse Density in 2D Confocal Images from Fixed Immunolabeled Neural Tissue Sections. *Methods in molecular biology (Clifton, N.J* 2040:71-97.

Supplemental Methods and Data

for

Neutrophil Extracellular Traps Drive Inflammation in Local Skin and Distant Kidneys in UVB-Irradiated Lupus-Prone Mice

Xing Lyu[1,2,4], Minghui Yi[1,2,], Minghui Li[1,2,4], Ping L. Zhang[3], Wei Wei[,4], Victoria P. Werth[1,2*], Ming-Lin Liu[1,2*]

[1] Corporal Michael J. Crescenz VAMC, Philadelphia, PA, USA
[2] Department of Dermatology, Perelman School of Medicine, University of Pennsylvania, Philadelphia, PA, USA
[3] Division of Anatomic Pathology, Beaumont Laboratories, Beaumont Health, Royal Oak, Michigan 48073, USA
[4] Department of Rheumatology and Immunology, Tianjin Medical University General Hospital, Tianjin, China

Short title: NETosis drives UVB-induced lupus skin and kidney inflammation

Correspondence to: Ming-Lin Liu, MBBS, PhD, and Victoria P. Werth, MD, Department of Dermatology, Perelman School of Medicine, University of Pennsylvania, and Philadelphia Veterans Administration Medical center. Room B414, 3900 Woodland Avenue, Philadelphia, PA 19104, eMAIL: lium1@pennmedicine.upenn.edu; werth@pennmedicine.upenn.edu

Key words: SLE, NETosis, PKCα, CXCR4, Skin-kidney communication,

Supplemental Data

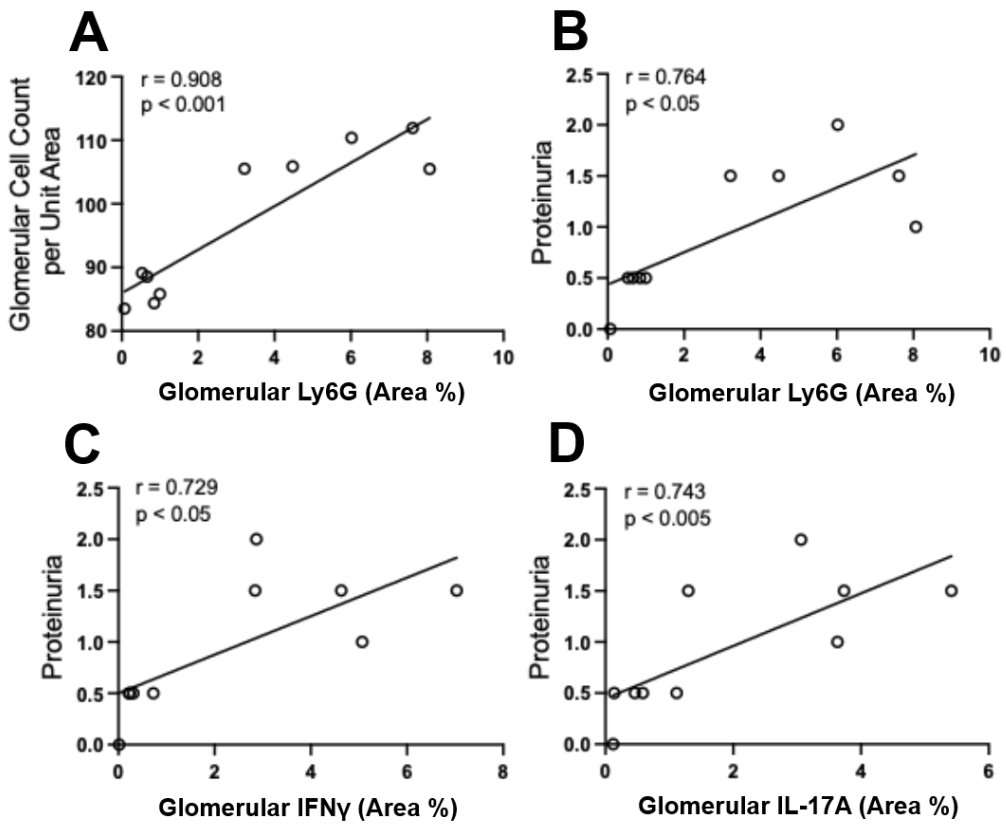

Suppl Fig 1. Renal neutrophil infiltration and NET-associated cytokines correlate with proteinuria in acute kidney inflammation in lupus-prone mice triggered by UVB. A. Correlation between glomerular neutrophil infiltration and glomerular cellularity. **B-D**. Correlation between glomerular neutrophils, NET-associated IFNγ, IL-17A with proteinuria in combined experimental groups. All data were analyzed using Pearson correlation coefficients.

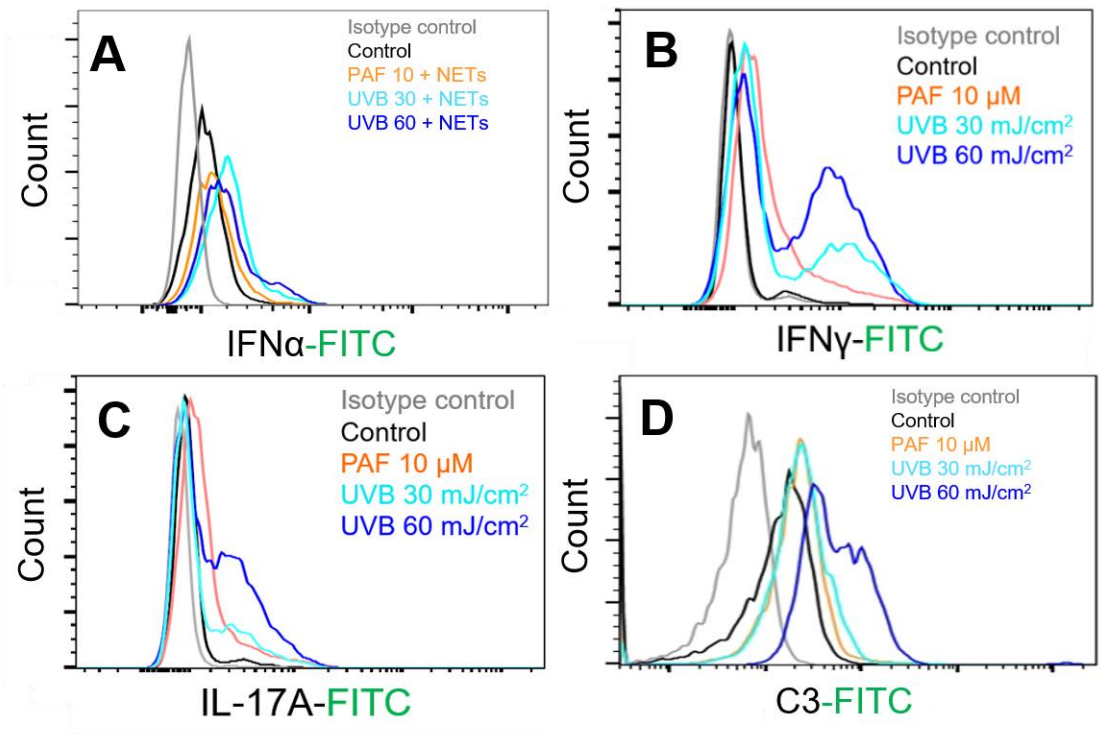

Suppl Fig 2. UVB induced expression of cytokines and C3 *in vitro* in primary neutrophils from lupus-prone mice. A-D. Representative histogram of IFNα, IFNγ, IL-17A, or C3 expression in primary neutrophils from lupus-prone mice. Cells were stimulated without (control) or with 10 μM PAF, or 30-60 mJ/cm^2 UVB irradiation, and incubated for 20h, then processed and immunostained as detailed in methods and Fig 5.

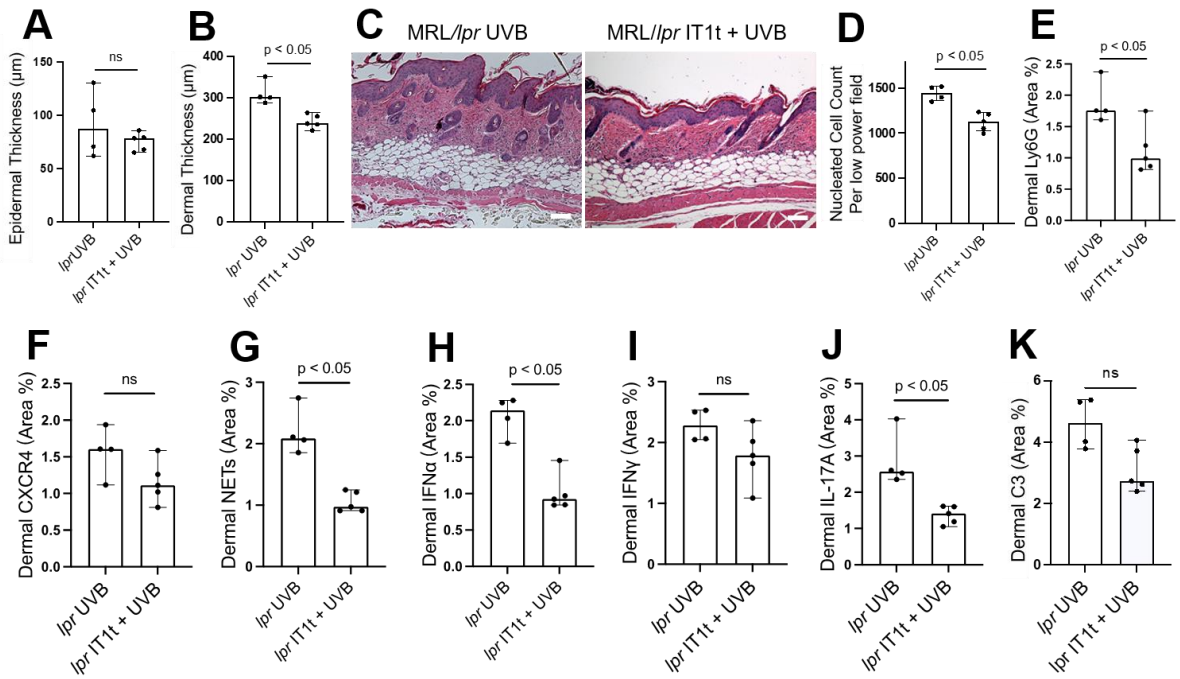

Suppl Fig 3. Effects of pharmacological CXCR4 inhibition on acute skin and kidney inflammation in UVB-irradiated lupus-prone mice. A-K. Summary analyses or representative H&E images of epidermal (A) and dermal (B) thickness, inflammatory cell infiltration (C-D, nucleated cells), neutrophils (E), CXCR4-expressing neutrophils (F), NETs (G), and NET-associated IFNα (H), IFNγ (I), IL-17A (J), or C3 (K) in skin of UVB-irradiated MRL/*lpr* mice without (lpr UVB) or with IT1t administration (lpr IT1t+UVB). Scale bars, 100 µm. Results represent 4-5 biological replicates. Panels A,B,D-K display means ± SD determined by student's t-test for two-group comparisons.